



Preliminary surficial geologic map of the Mesquite Lake 30' X 60' quadrangle, California and Nevada

By Kevin M. Schmidt and Matthew McMackin

Open-File Report 2006-1035

U.S. Department of the Interior
U.S. Geological Survey

U.S. Department of the Interior
Gale A. Norton, Secretary

U.S. Geological Survey
P. Patrick Leahy, Acting Director

U.S. Geological Survey, Reston, Virginia 2006
Revised and reprinted: 2006

For product and ordering information:
World Wide Web: <http://www.usgs.gov/pubprod>
Telephone: 1-888-ASK-USGS

For more information on the USGS—the Federal source for science about the Earth,
its natural and living resources, natural hazards, and the environment:
World Wide Web: <http://www.usgs.gov>
Telephone: 1-888-ASK-USGS

Suggested citation:
Schmidt, K.M., McMackin, M., 2006, **Preliminary surficial geologic map of the Mesquite
Lake 30' X 60' quadrangle, California and Nevada**: U.S. Geological Survey Open-File
Report 2006-1035, 89 p.

Any use of trade, product, or firm names is for descriptive purposes only and does not imply
endorsement by the U.S. Government.

Although this report is in the public domain, permission must be secured from the individual
copyright owners to reproduce any copyrighted material contained within this report.

Contents

Contents	iii
Abstract.....	8
Introduction.....	8
Physiographic Setting	11
Previous Mapping and General Geologic Framework	12
Methods	16
Quaternary units and geomorphic processes	17
Rock type, weathering, and hillslope processes	17
Alluvial processes.....	20
Eolian processes	24
Groundwater processes	25
Biologic processes	28
Quaternary Tectonics	29
Summary	33
Acknowledgements	34
Description of Map Units	34
Surficial Deposits	35
Anthropogenic deposits	35
Axial valley deposits	35
Wash deposits.....	36
Alluvial and debris-flow deposits	36
Eolian deposits.....	40
Mixed alluvial and eolian deposits	41
Playa deposits.....	42
Groundwater discharge deposits.....	44
Erosional surfaces and deposits on erosional surfaces	45
Hillslope environment	45
Pediment surfaces.....	46
Bedrock substrate materials (Tertiary and older).....	47
Composite symbols.....	48
References Cited	48

Figures

1. Regional topography in hillshade of study area with 30' X 60' Mesquite Lake quadrangle boundary shown as white rectangle. Roads are depicted in orange, major valleys labeled in yellow, California, Nevada, and Arizona state lines as white lines, and Mojave National Preserve boundary in red. The state line separates San Bernardino and Inyo Counties in California from Clark County in Nevada..... 56

2. Hillshade topography of Mesquite Lake 30' X 60' Mesquite Lake quadrangle showing principal geographic features in yellow, main roads in orange, primary drainage divides in blue, the California-Nevada state line in white, and the Mojave National Preserve in red.....	57
3. Authorship boundaries of mapping extent within 30' X 60' Mesquite Lake quadrangle. Orange line separates authorship with GPS waypoints collected by McMackin as blue dots and by Schmidt as red crosses. Stateline included as reference white line.....	58
4. View ~ 250° of Qoa (~6 m thick) overlying carbonate and siliciclastic bedrock (reddish sandstone) in middleground and the southern Bird Spring Range in background.....	59
5. View approximately south of exposed (Qhs) and colluvially mantled (Qha) Kingston Peak Formation granite near Tecopa Pass in the Kingston Range.....	60
6. Mid Holocene aged deposit composed of equigranular grus dominated by potassium feldspar overlying silty sandy A horizon largely devoid of vesicles. Ruler with color scale on whiteboard is ~ 10 cm long.....	61
7. Active boulders deposited by debris-flow processes under dashboard and steering column of abandoned vehicle east of Tecopa Pass in Kingston Range.....	62
8. Schmidt Hammer Values of Kingston Peak granite depicting decrease in strength of surface hardness as initially unvarnished outcrops become varnished and weather to grus. Upper plot depicts all measured sites separately while lower plot depicts averaged values for younger unvarnished and older varnished outcrops. Each vertically oriented rectangle encloses 50% of the data with the median value of the variable displayed as a horizontal line and the top (upper quartile) and bottom of the box (lower quartile) mark the interquartile distance.....	63
9. View approximately south of a balanced boulder as evidence for debris-flow transport in proximal fan within Kingston Range, near Crystal Spring.....	64
10. Pronounced chemical weathering of calcium carbonate clast forming solution cavities at surface of Qoa deposit, note 6 inch (15 cm) clear ruler for scale left of notebook. Effective surface lowering measured between solution cavity depths roughly parallel to present deposit surface and highest point on boulder is ~ 8 cm.....	65
11. Roughly planar stage IV B _{km} horizon exposed at surface and covered by thin disaggregated pavement of Qoa deposit. Note 15 cm long hand-held GPS unit for scale.....	66
12. Mid Pleistocene alluvial deposit (Qia) composed of carbonate bedrock clasts overlying silty A _v horizon ~ 7 cm thick. Note relative lack of desert varnish on moderately interlocking pavement clasts.....	67
13. View to the south showing the northwest Kingston Range piedmont with a late Pleistocene alluvium (Qia) veneer over stage IV carbonate-cemented B _{km} horizon from older alluvium.....	68
14. Moderately varnished mid Pleistocene (Qia) pavement composed primarily of carbonate clasts with minor volcanic clasts. Note prismatic soil structure of A _v ped to right of shallow soil pit with knife in shadow.....	69
15. Mid Holocene age alluvial deposit composed of randomly structured calcium carbonate bedrock clasts overlying sandy, silty, loose and unstructured A horizon. The unit potentially represents increased eolian fine material derived from nearby Roach Lake playa.....	70
16. View west in Kingston Wash of active channel (Qaa) inset within Qia/pc deposit.....	71

17. View roughly north of small active channel (Qaag) inset within Qiag deposit near Colosseum Gorge northeast of Clark Mtn. Note reddish brown B _w horizon and stage III B _{km} horizon in Qiag.	72
18. View along northbound direction of Interstate 15 traffic heading into dust storm on Ivanpah and Roach Lake playas on April 15, 2002 with Primm, Nevada in background.....	73
19. View 260° of active sand ramps climbing onto basalt (Qaer/mv) of McCollough Range near Hidden Valley. Foreground units dominated by young alluvium (Qya) and mixed eolian-alluvial deposits (Qyea).....	74
20. View northwest from Stateline Pass of active dust storm on Mesquite Lake playa.	75
21. View north of deflated sand dunes on east edge of Mesquite Lake playa. Note Qia soil exposed at base of mesquite topped dunes. Eolian deflation has lowered surface exposing gypsiferous playa sediments in lower left side marked by Atriplex.....	76
22. View northwest of Roach Lake playa, Interstate 15, and the southern Spring Mountains on March 21, 2001 with shallow standing water over typically dry playa surface (Qap).	77
23. View southeast of active dust storm from Roach Lake playa on March 25, 2001 with Lucy Gray Mountains and McCullough Range in background. Note, photograph of dust storm was taken four days after water observed on playa surface making roads across the playa surface impassable (fig. 20).	78
24. Gypsum-rich sediment exposed by deflation of Mesquite Lake bed. Elongate crystalline gypsum is overlain by progressively thicker, horizontal laminated mud toward the seasonal wetland on the floor of active Mesquite Valley wet playa sediment (Qapw).....	79
25. Bed of crystalline gypsum of the crystal body playa unit in Mesquite Lake Valley. In this view the upper bed, about 1 meter, is composed of approximately 60% intergrown gypsum crystals and 40% mud. Such crystal bed typically form below the surface and in this case are exposed in the uplifted of a fault transects the Mesquite Lake Basin (J, fig. 28). ...	80
26. Young playa fringe deposit (Qypf) on the west side of the Mesquite Lake Basin with a buried soil overlain by alluvial sand of a distal fan from the Mesquite Mountains. The whole section is cemented with gypsum precipitated by ground water discharge.	81
27. Mid Holocene deposit (Qya3) with heavy lichen cover with black, dark brown, and pinkish color. Clasts dominated by carbonate with some volcanic source rock.	82
28. Hillshade topography depicting faults, lineaments, and folds presented in plate 1 and table 1. Faults in red, lineaments in black, and fold axes in dashed black line.....	83
29. Truncated Qoa deposit (middle ground) with ~ 2 m of projected separation above Qia deposit (foreground). Note, break in slope at potential fault location also corresponds to only a 1 m separation between different bedrock types (ca and sl) exposed in channel cuts.	84
30. (A) Southeast oriented regional view of topographically back-facing talus slopes (Qoa in age) and broad topographic saddle in bedrock of Bird Spring Range. (B) Southeast oriented close-up view of topographically back-facing talus slopes (Qoa in age). Source region for talus slopes is currently separated by subtle topographic depression.....	85
31. Fault cutting older Quaternary sand deposits (Qoe) exposed in side canyon of Kingston Wash near Coyote Holes Spring. One meter tall boy for scale.	86
32. Carbonate-cemented faults cutting older Quaternary alluvium (Qoa) overlain by ~ 1 m of unfaulted mid and late Pleistocene (Qia) alluvial deposits. One of many faults exposed in a	

zone straddling the north fork of Kingston Wash (I, fig. 28). One-half meter tall meter dog stands on a Qia surface for scale. 87

Tables

Table 1. Characteristics of tectonic features, faults, folds, and lineaments, depicted in map on plate 1 and fig. 28. 88

Conversion Factors

Inch/Pound to SI

Multiply	By	To obtain
Length		
inch (in.)	2.54	centimeter (cm)
inch (in.)	25.4	millimeter (mm)
foot (ft)	0.3048	meter (m)
mile (mi)	1.609	kilometer (km)
yard (yd)	0.9144	meter (m)
Area		
square foot (ft ²)	929.0	square centimeter (cm ²)
square mile (mi ²)	2.590	square kilometer (km ²)
Volume		
quart (qt)	0.9464	liter (L)
gallon (gal)	3.785	liter (L)
gallon (gal)	0.003785	cubic meter (m ³)
Flow rate		
cubic foot per day (ft ³ /d)	0.02832	cubic meter per day (m ³ /d)
Mass		
pound, avoirdupois (lb)	0.4536	kilogram (kg)

Temperature in degrees Celsius (°C) may be converted to degrees Fahrenheit (°F) as follows:

$$^{\circ}\text{F}=(1.8\times^{\circ}\text{C})+32$$

Temperature in degrees Fahrenheit (°F) may be converted to degrees Celsius (°C) as follows:

$$^{\circ}\text{C}=(^{\circ}\text{F}-32)/1.8$$

Vertical coordinate information is referenced to the insert datum name (and abbreviation) here for instance, “North American Vertical Datum of 1988 (NAVD 88).”

Horizontal coordinate information is referenced to the insert datum name (and abbreviation) here for instance, “North American Datum of 1983 (NAD 83).”

Altitude, as used in this report, refers to distance above the vertical datum.

SI to Inch/Pound

Multiply	By	To obtain
Length		
centimeter (cm)	0.3937	inch (in.)
millimeter (mm)	0.03937	inch (in.)
meter (m)	3.281	foot (ft)
kilometer (km)	0.6214	mile (mi)
meter (m)	1.094	yard (yd)
Area		
square centimeter (cm ²)	0.1550	square inch (ft ²)
square kilometer (km ²)	0.3861	square mile (mi ²)
Volume		
liter (L)	1.057	quart (qt)
liter (L)	0.2642	gallon (gal)
cubic meter (m ³)	264.2	gallon (gal)
Flow rate		
gallon per day (gal/d)	0.003785	cubic meter per day (m ³ /d)
Mass		
kilogram (kg)	2.205	pound avoirdupois (lb)

Temperature in degrees Celsius (°C) may be converted to degrees Fahrenheit (°F) as follows:

$$^{\circ}\text{F}=(1.8\times^{\circ}\text{C})+32$$

Temperature in degrees Fahrenheit (°F) may be converted to degrees Celsius (°C) as follows:

$$^{\circ}\text{C}=(^{\circ}\text{F}-32)/1.8$$

Vertical coordinate information is referenced to the insert datum name (and abbreviation) here, for instance, “North American Vertical Datum of 1988 (NAVD 88)”

Horizontal coordinate information is referenced to the insert datum name (and abbreviation) here, for instance, “North American Datum of 1983 (NAD 83)”

Altitude, as used in this report, refers to distance above the vertical datum.

Preliminary surficial geologic map of the Mesquite Lake 30' X 60' quadrangle, California and Nevada

By Kevin M. Schmidt¹ and Matthew McMackin²

Abstract

The Quaternary surficial geologic map of the Mesquite Lake, California-Nevada 30'X60' quadrangle depicts deposit age and geomorphic processes of erosion and deposition, as identified by a composite of remote sensing investigations, laboratory analyses, and field work, in the arid to semi-arid Mojave Desert area, straddling the California-Nevada border. Mapping was motivated by the need to address pressing scientific and social issues such as understanding and predicting the effects of climate and associated hydrologic changes, human impacts on landscapes, ecosystem function, and natural hazards at a regional scale. As the map area lies just to the south of Las Vegas, Nevada, a rapidly expanding urban center, land use pressures and the need for additional construction materials are forecasted for the region. The map contains information on the temporal and spatial patterns of surface processes and hazards that can be used to model specific landscape applications. Key features of the geologic map include: (1) spatially extensive Holocene alluvial deposits that compose the bulk of Quaternary units (~25%), (2) remote sensing and field studies that identified fault scarps or queried faults in the Kingston Wash area, Shadow Mountains, southern Pahrump Valley, Bird Spring Range, Lucy Gray Mountains and Piute Valley, (3) a lineament indicative of potential fault offset is located in Mesquite Valley, (4) active eolian dunes and sand ramps located on the east side of Mesquite, Ivanpah, and Hidden Valleys adjacent to playas, (4) groundwater discharge deposits in southern Pahrump Valley, Spring Mountains, and Lucy Gray Mountains and (5) debris-flow deposits spanning almost the entire Quaternary period in age.

Introduction

The geologic map of the Mesquite Lake 1:100,000 scale quadrangle, lies in the north-eastern portion of the Mojave Desert, north of the Mojave National Preserve, and is bisected by the state line including portions of San Bernardino and Inyo Counties (California) and Clark County (Nevada) (figs. 1 and 2). As part of a larger U. S. Geological Survey (USGS) campaign to map surficial deposits within the arid Southwest of the United States, including the Basin and Range, Mojave, Sonoran, and Colorado Plateau Provinces, mapping in the 30'X60' Mesquite Lake quadrangle is largely reconnaissance in nature but supported by considerable field

¹ U.S. Geological Survey, 345 Middlefield Rd, MS 973, Menlo Park, CA 94025

² San Jose State University, Dept. of Geology, One Washington Square, San Jose, CA 95112

observations (fig. 3). Geologic units in the area are diverse consisting of Proterozoic granitoids and metamorphic rocks, Paleozoic sedimentary rocks, Tertiary granitoids, extrusive volcanic flows, and basin fill, as well as Quaternary surficial deposits. The map depicts regional characteristics of Quaternary deposits with bedrock units generalized with respect to bulk composition. Quaternary surficial deposits are classified into soil-geomorphic surfaces based on soil characteristics, inset relationships, geomorphic expression, and genetic processes of erosion and deposition. Bedrock is here described by compositional, textural, and stratigraphic relationships with implications for the generation and character of surficial material.

Relative and absolute deposit age of surficial material has been closely correlated with pedogenic maturity in the Mojave Desert region (Denny, 1965; Machette, 1985; Wells and others, 1985; McFadden and others, 1987; Wells and McFadden, 1987; McFadden and others, 1989; Reheis and others, 1989; Yount and others, 1994; Reheis and others, 1996; Birkeland, 1999; McDonald and others, 2003). Reheis and others (1989), for example, used well-dated deposits at Silver Lake, to the west of our study area, to calibrate changes in pedogenic maturity throughout a late Pleistocene to modern depositional sequence. These prior studies document that recent and young deposits are relatively devoid of strong pedogenic development. In contrast, Pleistocene-aged deposits display a diagnostic soil sequence including an interlocking surface pavement of clasts (e.g., Cooke, 1970) directly underlain by a pale-colored, vesicular, silt-rich A_v horizon (or A_{vk} horizon; where k indicates an accumulation of calcium carbonate) (McFadden and others, 1986, 1987, 1998). Using soil-stratigraphic and geochemical data, McFadden and others (1986, 1987, 1998) demonstrated that eolian dust accumulates below surface clasts of an evolving one- to two-particle thick, varnished, stone pavement layer of closely packed clasts to form a clayey argillic horizon (A_v). These desert pavement characteristics have been used for decades to map relative ages of Quaternary surficial deposits (e.g., Denny, 1965). In advanced soil chronosequences, reddish, cambic (B_w), argillic (B_t), or calcium carbonate rich reddish, cambic or argillic (B_{wk} or B_{tk} , respectively) horizons lie below the A_v horizon, representing illuviated fine particles and iron oxidation. The B_w horizon is identified based upon the development of a reddish color with little illuviation of material (Birkeland and others, 1991). The argillic horizon (B_t), in contrast, is identified on the basis of larger quantities of illuviated or translocated silt and clay, exhibits a brown to reddish color, and commonly displays clay films (McFadden and others, 1986; Birkeland and others, 1991). At the base of the B horizon subunits lies the B_{km} horizon, a massive horizon impregnated with calcium carbonate. As a measure of the maturity of pedogenic and cryptalgal features in the B_{km} horizon, Gile and others (1965) developed a classification scheme which Machette (1985) modified to describe whether the authigenic carbonate merely coats or completely engulfs nearly all the grains as a continuous medium. Although many soil chronosequences exist to describe the varying degrees of soil development discussed above related to deposit age, the framework adopted here relies largely on that proposed by Yount and others (1994), but includes the process understanding of desert soil morphogenesis described in McFadden and others (1998).

The map represents both relative Quaternary deposit ages and genetic formation processes, hence geomorphically active regions prone to specific natural hazards and landscape characteristics of critical environmental concern can be delineated. Surficial geologic maps, particularly when combined with physical property databases, are multipurpose and are needed to evaluate compaction susceptibility from vehicle traffic, isolate areas of active tectonics, identify

sites of eolian erosion/deposition and dust emission, and constrain flood and debris-flow frequency/magnitude relationships. Aerial extents of mapped features provide first order estimates of source regions, volumes of sediment mobilized, and areas of inundation. As Quaternary deposits are tightly coupled to tectonic, climatic, and hydrologic processes, the sedimentary sequences record information about past conditions, which in turn can be used to infer possible consequences of future conditions such as climate variability on natural hazard susceptibility.

As the genetic process and relative age of the materials imparts a strong influence on the deposit character, surficial geology provides a template to define and extrapolate, physical properties influencing surface characteristics (McFadden and others, 1987, 1998), run-off generation (Schlesinger and others, 1989), and soil-water-plant dynamics (Hammerlynck and others, 2002). The physical properties of sediments such as desert pavement development, pedogenesis, and hydraulic characteristics strongly influence the availability of water and nutrients for biota; information that is vital for predicting ecosystem function, health, and recoverability from disturbance. Availability of soil moisture is critical because it affects most landscape resources through biogeochemical cycling rates and processes (Hammerlynck and others, 2002). As geologic deposit age strongly influences material properties such as particle size distribution, bulk density, and chemical constituents, the spatial distribution of surficial units differentially affects soil moisture and nutrient availability. Previous studies have noted that soil horizon development and depositional process are related to vegetation species composition and density (Webb and others, 1987; McAuliffe, 1994; McAuliffe and McDonald, 1995; Steiger and Webb, 2000; Hammerlynck and others, 2002). Furthermore, the recovery of ecosystems to anthropogenic disturbance, in the eastern Mojave Desert and other arid- semi-arid environments, is also tied to physical characteristics of surficial deposit age and process (e.g., Webb and others, 1988; McAuliffe and McDonald, 1995; Steiger and Webb, 2000; Belnap and others, 2001). Webb and others (1988) and Steiger and Webb (2000), for example, determined that inverse relations exist between the rate of post-disturbance revegetation and the degree of soil development or deposit age. More specifically, characteristics of a given soil horizon may dictate hydrologic conditions and hence vegetation suitability. For instance, the influence of calcium carbonate rich deposits (B_{km} horizons) on desert plants could be wide ranging in that it may provide physical barriers to vegetation root growth as well as influence hydrologic flow paths, soil moisture, and runoff frequency. Besides being a partial barrier to both upward and downward soil moisture migration, excavations by Shreve and Mallery (1933) revealed that roots did not penetrate B_{km} horizons, but rather extended horizontally along the surface for as much as 3 to 5 m. McDonald and others (1996) suggest that soil water only reaches the lower zone of carbonate horizons of older deposits during wet years of the current climate. Alternatively, coarse-textured, weakly developed soils of more recent deposits allow for deeper infiltration of water with correspondingly larger canopy volumes of certain plants (Hammerlynck and others, 2002).

The relative availability of soil moisture, as modified by geologic deposit type and age, influences a wide range of landscape response characteristics including vegetation cover, eolian transport, surface-water routing and sediment transport, as well as fire frequency and severity. For example, remobilization of particularly sensitive environments such as existing eolian deposits or playa fringes can occur by destabilizing or converting vegetation in response to decreased soil moisture. In addition, regional evaluations of alluvial fan deposition have been

hindered by a lack of surficial geologic mapping, representative sediment transport relations, and stratigraphic correlations among fan deposits across different geomorphic settings. Hence, documenting the aerial distribution of surficial geologic deposits and their associated physical and hydrological properties will likely lead to refined understanding of unsaturated soil moisture availability, rainfall/runoff characteristics, and the distribution of vegetation assemblages.

Physiographic Setting

The landscape is comprised of physical features characteristic of the southern Basin and Range, though botanically the area is considered part of the Mojave Desert (Spaulding, 1990), with select Sonoran species locally present. Tectonic and structural controls provide the first order influence on topography, drainage basin characteristics, and vegetation assemblages in the map area. Generally northwest-trending, semi-arid, high-relief mountain ranges of various rock types and dimension separate arid broad alluviated piedmonts with alluvial fan deposits grading into fine-grained sediments on the valley floor, typically occupied by playas (Fig. 2). Bedrock ranges, such as the Spring Mountains, generally exhibit high relief with deeply embayed canyons that issue to a mixture of traction (fluvial) and inertial (debris flow) dominated alluvial fans along the range front. Moderately sloping medial fan deposits, comprising the largest surface area of Quaternary deposits, are redistributed by intra-fan drainage driven by local run-off during intense or long duration rainfall. Moderately to gently sloping distal-fan sediments are typically reworked by braided alluvial channels as well as by the possible addition of eolian sand and sediments associated with groundwater discharge. The valley floors are composed of fine-grained sediments that form wet groundwater discharge playas or dry playa lake deposits. Regionally, topographically complex landscapes encompass different climatic domains reflecting differences in elevation, slope angle and aspect, source rock composition and texture, among other factors. Locally, vegetation responds to climate via interaction with the amount and timing of soil moisture, temperature, humidity, and available nutrients.

The mean annual precipitation is typically <200 mm falling mostly as sporadic discontinuous rain, with amounts generally increasing with elevation (French, 1983), and snow accumulating at higher elevations in the winter. Snow is common in higher elevations of the Kingston Range, Spring Mountains, Clark Mountains, and McCullough Range and may remain on the ground for much of the winter season. Runoff is rapid from hillslopes and alluvial fans with surface flow in channels only occurring after intense localized precipitation. Temperatures in the region are extreme with cold winters accompanied by sporadic rainfall from Pacific frontal storms and hot, dry summers with highly infrequent, but occasionally intense monsoonal convective storms.

Areas of high topographic relief, such as the Spring Mountains, McCullough Range, Clark Mountains, and Kingston Range, all reach elevations over 2100 m above sea level and support vegetation characterized by singleleaf pinyon (*Pinus monophylla*) and white fir (*Abies concolor*). In the Kingston Range, agave (*Nolina wolfii*) is common at elevations above 1300 m and California barrel cacti (*Ferocactus cylindraceus*) are particularly abundant. Plant macrofossil assemblages preserved within packrat middens located within the McCullough Range record an increase in species richness, as measured by the number of taxa, from the middle to late Holocene (Spaulding, 1990). Interposition of different vegetation zones such as common on high-relief

topography, though, may create barriers to migrating biotic niches. Downslope of the bedrock uplands, piedmonts of gently to moderately sloping alluvial fans lead to nearly level basins with elevations of 500 to 800 m. In the valley floors, bedrock is generally overlain by Quaternary alluvium transported by a combination of streamflow, sheetflow, and mass wasting processes. At intermediate to upper piedmont elevations, vegetation assemblages are dominated by blackbrush (*Coleogyne ramosissima*) and Joshua Tree (*Yucca brevifolia*). At lower elevations on the alluvial fans, vegetation assemblages are dominated by small shrubs such as creosote bush (*Larrea tridentata*), white bursage (*Ambrosia dumosa*), and plants in the Agave Family such as yuccas. Vegetation common to lower elevation valleys and channels includes catclaw (*Acacia greggii* var. *arizonica*), mesquite, black-banded rabbitbrush (*Chrysothamnus paniculatus*), desert willow (*Chilopsis linearis*), and locally smoke tree (*Psoralea argophylla*).

Watershed boundaries in the map area can be divided into two primary domains; internally and externally drained valleys (Fig. 2). Examples of internally drained valleys are Pahrump, Mesquite, Eldorado, and Ivanpah Valleys. They are largely sourced from carbonate and plutonic bedrock watersheds that route surface water along valley axes to local playas in topographic lows. Kingston Wash and upper California Valley near the western edge of the quadrangle, are also internally drained, but water is routed to the Death Valley sink. Surface flow in Kingston Wash enters by intersection with the Mojave River and California Valley by way of the Amargosa River system. The externally drained systems are Piute Valley and portions of the Spring Mountains. The present day Piute Valley drainage divide in the southeast portion of the quadrangle, separating south-flowing drainage into the Lower Colorado River, is controlled by an east-west trending structural anticline through the Highland Spring Range, as recognized by Hewett (1956) and here inferred from field relations of deposit age, gradient, and orientation of deposition. The watershed boundary in the northeast part of figure 2 incorporates drainages from the east slope of the southern Spring Mountains and the Bird Spring Range that also connect to the Colorado River basin through Las Vegas Wash.

Previous Mapping and General Geologic Framework

Economic bedrock geology motivated most of the earliest existing geologic mapping and bedrock stratigraphy studies in the region (e.g., Hill, 1914; Hewett 1931, 1956). Similarly, Wright and others (1953) and Wright (1968) chronicled the mineral resources throughout San Bernardino County and Jennings and others (1962) depicted regional bedrock geology in a California state compilation. Expanding on the work of Hewett (1956), Bowyer and others (1958) and Longwell and others (1965) produced maps and detailed discussions of the mineral deposits of Clark County. A combination of economic geology and tectonic studies focused considerable research within the Paleozoic carbonate-dominated bedrock of the southern Spring Mountains and the mixed Precambrian crystalline and Paleozoic to Mesozoic sedimentary bedrock of the Clark Mountains (Hewett, 1931; Albritton and others, 1954; Clary, 1967; Burchfiel and Davis, 1971; Carr, 1980, 1983; Carr and Pinkston, 1987; Fleck and others, 1994; Walker and others, 1995). In the McClanahan mining district of the McCullough Range, Bingler and Bonham (1972) mapped bedrock geology whereas DeWitt and others (1989) examined the mineral resource potential of the Proterozoic granitic and gneissic rocks overlain by Tertiary mafic volcanics. Calzia and others (1987) discussed the mineral resource potential (largely talc and iron skarn) of the rock units surrounding the Miocene Kingston Range pluton whereas Calzia and others (2000) published a

geologic map compilation of the entire range, emphasizing features related to mid-Miocene crustal extension. Although no existing published surficial geologic maps existed prior to the onset of this mapping effort, the Nevada Bureau of Mines and Geology (NBMG) began and produced a number of 1:24,000 scale maps along the Interstate Highway 15 corridor (House and Park, 2003; Ramelli and others, 2003; House, 2004; House and others, 2004; Ramelli and others, 2004a, 2004b). The geologic unit nomenclature adopted by NBMG was modified from that used here by the regional USGS mapping effort. The parallel mapping efforts are similar in regional features, but differ in detail because of map scale.

The Mesquite Lake quadrangle lies at a complicated intersection of tectonic provinces that changed through time, and as such, the bedrock is stratigraphically diverse and structurally complex (Hewett, 1956; Longwell and others, 1965) with mountain range orientations and local relief influencing the regional drainage framework and upland sediment sources for the widespread alluvial fans (fig. 2). The map of Hewett (1956), encompassing the entire Mesquite Lake quadrangle, depicts the transition from Precambrian crystalline rocks in the east, to Paleozoic and Mesozoic sedimentary rocks to the west. This transition corresponds roughly with the location of Interstate Highway 15, although carbonate rocks are present as far east as Sheep Mountain near Jean, Nevada. The carbonate-dominated sequence west of Interstate Highway 15, consisting of limestone, dolomite, and calcareous clastic units, was deposited along a passive Paleozoic continental margin and was deformed during the Mesozoic when the margin became tectonically active. The primary structural features of Mesozoic deformation, such as faults and folds, not only influence the topographic features of the region, but also the spatial distribution of rock types. For example, the eastern margin of the Mesozoic Cordilleran Sevier orogenic belt extending from Canada to southeastern California (e.g., Armstrong, 1968; Fleck, 1970; Burchfiel and Davis, 1971; Burchfiel and others, 1974) dictates the distribution of rock types. Although the specifics of timing and kinematics of deformation are debated, the Spring and Clark Mountains represent the southernmost characteristic Cordilleran tectonics where the Paleozoic miogeoclinal sedimentary sequences were deformed by Mesozoic east-vergent thrusting and folding (e.g., Fleck, 1970; Burchfiel and others, 1974; Carr, 1983). These west-dipping thrust faults superimposed marine carbonate rocks over roughly coeval rocks of more cratonal facies. Traversing the entire length of the Spring Mountains for nearly 70 km, the Keystone thrust is the primary miogeocline-craton boundary with a maximum age of emplacement dating to late Early Cretaceous (Fleck and Carr, 1990). To the south, Walker and others (1995) constrained the initiation of this fold-and-thrust belt in the Clark Mountains to Late Jurassic time and Fleck and others (1994) argue deformation continued to at least the late Early Cretaceous. Although minimum ages of deformation are poorly constrained due to a lack of younger strata, local outcrops of Tertiary volcanic and sedimentary sections unconformably overlie these previously deformed Proterozoic and carbonate-dominated Paleozoic rocks. To the southwest of the quadrangle lies the Mojave Desert block characterized by Mesozoic magmatic arc rocks deformed by Cenozoic strike-slip faults (e.g., Dokka, 1989; Dokka and Travis, 1990; Glazner and others, 2002).

The present topography is typified by generally north-northwest trending, sub-parallel ranges separated by alluvial basins of similar plan and orientation. This classic Basin and Range physiography is the product of polygenetic middle to late Cenozoic deformation, where ranges are at least partly bounded by west-vergent, listric or shallowly dipping normal faults and associated

strike-slip faults characteristic of the Basin and Range province (e.g., Wernicke and others, 1988). Although the Spring and Clark Mountains within the Mesquite Lake map area are anomalously unaffected by this extensional deformation (Burchfiel and others, 1974; Jones and others, 1992), to the north of the study area at the latitude of Las Vegas, Nevada, the Basin and Range province has undergone substantial extension (a factor of up to 3 to 4) during the last 15 M.y. (Wernicke and others, 1988) resulting in topographically high mountains. In the Highland Range, thick tilted sections of Miocene volcanic and sedimentary strata accumulated immediately prior to and during regional extension which Faulds and others (2002) used $^{40}\text{Ar}/^{39}\text{Ar}$ dating techniques to bracket major extension between about 16.5 and 11 Ma. Similarly, the andesitic and basaltic volcanic rocks in the McCullough Pass area of the McCullough Mountains have been dated by $^{40}\text{Ar}/^{39}\text{Ar}$ techniques from 13.1 to 15.6 Ma (Faulds and others, 1999). To the west of the Clark Mountains, the Shadow Valley region and the Kingston Range have also undergone Neogene extension along southwest-vergent detachment faults (McMackin, 1988; Wernicke and others, 1988; Jones and others, 1992; McMackin, 1992; Davis and others, 1993; Kaufman and Royden, 1994). Linkages between faulting, topography, source rocks, and basin sedimentation have been previously recognized along this western margin of the map area. For example, Davis and others (1993) suggested the steep topography of Mountain Pass and the Clark and Mesquite Mountains results from the breakaway zone of detachment faulting whereas the steep topography of the Kingston Range results from the intrusion of the Kingston Peak pluton along a portion of the Kingston Range-Halloran Hills detachment fault system and uplift of its country rocks. Erosion of the pre-pluton country rocks produced the voluminous Shadow Valley basin fill— consisting of syntectonic Miocene alluvial sequences located in the upper plate of the detachment. Intrusion of the Kingston Peak pluton across the detachment fault likely terminated displacement at deeper levels around 12.6 ± 0.5 Ma based on zircon fission track analyses or 12.4 ± 0.04 Ma based on $^{40}\text{Ar}/^{39}\text{Ar}$ dating (Fowler and Calzia, 1999). The pluton was unroofed rapidly as indicated by the apatite fission track date of 9.1 ± 0.7 Ma (Topping, 1993) and the presence of Kingston Peak pluton detritus in nearby Miocene basins filled with up to 3 km of sediments (Friedmann and others, 1996; Friedmann 1999; Prave and McMackin, 1999). Friedmann and others (1996) and Friedmann (1999) examined the stratigraphy of the Shadow Valley basin sourced from the footwall of the Kingston Peak detachment and concluded that basin was a shallow broad depocenter composed chiefly of alluvial fan and lacustrine desposits with deposition rates as high as 0.5 mm/yr, while Topping (1993) proposed that this rapidly accumulating basinal sedimentary sequence represents massive unrooted rock-avalanche deposits.

In addition to Miocene normal faulting, Neogene strike-slip faults accommodated horizontal extension and possibly localized shortening (Wernicke and others, 1988; Jones and others, 1992; Davis and others, 1993). Prave and McMackin (1999) also highlight the role of strike-slip tectonism associated with extensional tectonism, typified by normal faulting, as a potential mechanism for development of Miocene basins such as the Shadow Valley basin. Supporting the role of strike-slip faulting in crustal deformation and the generation of topography, just north of the map area lies the Las Vegas Valley Shear zone, a northwest-striking fault zone with significant dextral displacement (Gianella and Callaghan, 1934; Longwell, 1960; Longwell and others, 1965; Langenheim and others, 2001) that intersects and offsets the Sevier orogenic belt. Through stratigraphic constraints, Stevens and others (1991) inferred 45-50 km of right-lateral offset on this shear zone. Applying geophysical methods, Langenheim and others (2001) inferred that deep sub-basins filled with alluvium and low-density deposits up to 5 km thick are

present along the shear zone. This inherited pre-Quaternary tectonic framework continues to influence the location of source material in bedrock uplands, the loci of deposition, and possibly the Quaternary patterns of tectonic deformation.

The primary Quaternary fault recognized in the map region is the southern extension of the Pahrump Valley fault zone, multiple traces of which are broadly aligned within Pahrump and Mesquite Valleys along the California-Nevada state border. Although Hoffard (1991), Anderson and others (1995), and McMackin (1999) documented Quaternary slip on the Pahrump Valley fault zone in southern Pahrump Valley (likely contiguous with the Stateline fault), there was little documented evidence for late Quaternary displacement within the Mesquite Lake quadrangle. Although bedrock exposures indicate significant strike-slip displacement, studies of Quaternary deposits provide low vertical slip rates near Stump Spring where the fault is overlain by late Pleistocene groundwater discharge deposits also described by Quade and others (1995). Detailed mapping by McMackin (1999) showed that pedogenic carbonate sealing fault scarps in the region of Black Butte is folded gently about northwest-trending axes that are sub-parallel to the fault zone, indicating younger tectonic deformation without surface rupture.

Hydrologic studies including climatic control on water resources (e.g., groundwater availability, springs, and playas) are a topic of great interest in this arid region. Although Hill (1914) focused on the Yellow Pine District (later publications refer to the region as Goodsprings District), Hill noted that the water supply in Mesquite Lake was abundant with a water table close to the surface and included similar descriptions of Ivanpah Valley: a “practically limitless supply of water can be obtained from wells 10 to 50 feet deep.” Maxey and Robinson (1947) provide a comprehensive examination of groundwater resources in the southern Las Vegas Valley region noting that the primary source for groundwater recharge in the region is precipitation from the Spring Mountains. Similarly, Malmberg (1967) noted that groundwater pumping, starting in 1910, relied upon ground water recharge from the Spring Mountains that was likely partitioned into a deep carbonate aquifer and shallower sedimentary fill in Pahrump Valley. He also noted the development of artesian wells in 1910 with later extensive pumping from the 1940’s to early 1960’s significantly depleted the valley fill reservoir. French (1983) presented intensity/duration precipitation data in the context of groundwater resources for southern Nevada while Turner (1990) analyzed stream and playa sediments with NURE (National Uranium Resource Evaluation) data. Quade and others (1995, 2003) noted that Quaternary fossil spring deposits, such as those studied in Mesquite and Pahrump Valleys, were historically misidentified as being lacustrine in origin. These spring deposits provide critical constraints on the hydrologic response of regional water tables to climate change. Increased recharge during pluvial periods in the Spring Mountains, for instance, caused groundwater to discharge over wide areas of Pahrump and Mesquite Valleys. Quade and others (1995) also recognized the potential importance of fault-control on groundwater discharge in these valleys. In Mesquite Valley, for example, faults and lineaments marked by phreatophytic mesquite (*Prosopis glandulosa*) denote areas where faults may have dammed local groundwater flow as recently as 11,020 ¹⁴C yr B.P. (Quade and others, 1995). Forester and others (1999) also acknowledge that paleo-hydrological information in Pahrump Valley likely reflects fault control on hydrologic conditions as the water table rises discontinuously along the valley bottom. Forester and others (1999), examining ostracode species and macrofossil data for sediments from former groundwater discharge deposits in Las Vegas Valley, inferred environmental depositional conditions that reflect a higher level of effective

moisture and a lower mean annual temperature than present conditions. These freshwater wetlands existed around 36 ka and persisted in some areas to about 12 ka.

Methods

Mapping was conducted during the period from 2001 to 2004 using a synergistic combination of field methods and interpretation of remotely sensed data. Analyses of remote sensing data included aerial photographs, Landsat7 data, digital orthophotograph quarter quadrangle (DOQQ), and digital elevation models. Absolute age dating of the spectrum of geologic units mapped was not possible due to a lack of suitable datable material, as well as time and funding constraints. Rather, a relative deposit age was determined to provide a temporal framework. Given that the sedimentology is similar within most alluvial deposits regardless of age, we used distinctive surface properties and pedogenic characteristics to delineate and correlate map units. Relative ages were differentiated by examining a combination of diagnostic criteria including: the geomorphic position, deposit surface roughness, drainage patterns, channel incision, degree of pavement maturity, pedogenic development, source lithology and degree of clast weathering, vegetation assemblages, and relative elevation (e.g., Christenson and Purcell, 1985; Bull, 1991). The chronosequence methodology adopted here is similar to Christenson and Purcell (1985) and Yount and others (1994). We determined pedogenic maturity by examining available channel and road cut exposures and by excavating shallow pits with a shovel to depths of roughly 0.5 m to estimate relative degrees of weathering and translocation of material. We evaluated the thickness of soil horizons such as the A_v, strength of the argillic horizon (B_v) or calcic (B_{tk} or B_{km}) as well as the occurrence of pedogenic and cryptalgal features in the caliche horizon. Undergoing primarily progressive development, the soils tend to become better differentiated by horizons, the horizon contrasts become greater, and the profile thickness tends to increase over time.

By comparing relative pedogenic development, we assume that soils throughout the map area formed under similar regional, environmental conditions taking into consideration those unique deposits subjected to rapid and excessive addition or removal of material hence altering the time-transgressive nature of soil formation. Assuming that factors such as climate, vegetation, topographic setting, and parent material are constant over time is likely erroneous for older, undoubtedly polygenetic soils. Undoubtedly climatic fluctuations altered rates of erosion and deposition but few well-dated deposits can be temporally linked to detailed climate records. Geomorphic controls likely influence climatically driven alluvial fan deposition rates as well. In addition, Reheis and others (1989) reported that variations in chronosequence designations occur when multiple individuals describe the same soil. As such, age designations for the units were determined independently by each author; such that McMackin was solely responsible for the western portion of the map and Schmidt was solely responsible for the eastern portion (fig. 3). Age and processes designations across authorship boundaries, both internal to this map and across 30'X60' quadrangles (e.g., Las Vegas quadrangle of Page and others, 2005 to north), were overall quite consistent but were locally edge matched by the authors where differences occurred.

Surficial unit boundaries are represented by identifying the lateral extent of continuous units based upon aerial photograph analyses by stereoscopic techniques, analyses of remote sensing images, as well as field examination of landforms, deposits, and soil development.

Typically map unit designation and spatial boundaries were derived from an iterative process of synergistic image analysis and field interpretation. All field observations were geo-located using a 10-channel, handheld global positioning system (GPS) with a NAD83 datum and a Universal Transverse Mercator (UTM) zone 11 projection. Field relations were also mapped in the field using DOQQ plots as base materials at scales of 1:24,000 to 1:12,000. Map unit boundaries drawn on aerial photographs using a stereoscope were "heads up" digitized using a geo-referenced DOQQ on a computer screen at a scale of roughly 1:15,000 to ensure accurate locations of line work denoting polygon boundaries and arcs.

Bedrock units were generalized into eight categories based upon chemical composition and weathering characteristics in accordance with the regional compilation of Bedford and Miller (1998) and Hewett (1956) with exact boundaries determined from field relations as well as analyses of aerial photographs, DOQQ's, and Landsat7 remote sensing images. In addition, bedrock unit descriptions in the western half of the quadrangle was taken largely from unpublished mapping by McMackin as well as Clary (1967).

Quaternary units and geomorphic processes

The map on plate 1 reveals a landscape composed of mountain ranges spanning a wide range of rock types, piedmonts dominated by alluvial fan deposits surrounding the bedrock ranges, and valley floors where fine-grained sediments accumulate in low-gradient, axial valley drainages and closed-basin playas. The following discussion of surficial deposits, generated from a suite of geomorphic processes, is presented in a decreasing potential energy of depositional process, source-to-sink framework.

Rock type, weathering, and hillslope processes

Bedrock composition influences the general appearance of the north-northwest oriented mountain ranges in the study area (Figures 1 and 2). Ranges composed largely of Paleozoic limestone and dolomite, such as the Spring Mountains, appear rugged with high relief and dark-gray ridges. As Hill (1914) and Hewitt (1956) noted, carbonate rocks common to Basin and Range Province, tend to resist erosion more than neighboring porphyritic igneous or siliceous sedimentary rocks. The resulting hillslopes of carbonate rocks tend to be steep and largely devoid of overlying colluvium. Complicating this relation, though, is the presence of mechanically weak interbeds. On the south side of the largely carbonate Bird Spring Range, for example, a specific combination of rock types, weathering, and sediment transport processes has generated a feature resembling a pediment such that the hillslopes are surrounded by a broad, relatively flat bedrock expanse covered with a thin alluvial mantle (fig. 4). This pediment-like feature likely exists because of the mechanically weak Permian "red beds" (Longwell and others, 1965) oriented with a shallow dip. Hillslopes underlain by such weak sedimentary rocks are more easily eroded and have more subdued morphology such that bedrock outcrops are often absent. Precambrian, relatively coarse-grained crystalline rocks of the southern McCullough Range and Kingston Range, in stark contrast, are irregularly dissected but express generally steep slopes and moderate to high-relief hillslopes. Alternatively, the northern McCullough and Highland Spring Ranges are

composed of Tertiary mafic volcanic rocks (largely andesite and basalt) that tend to weather as large blocks derived from moderate gradient and relief hillslopes.

In addition to modulating the landscape-scale appearance of the ranges, the distribution of bedrock source materials affects the resulting surficial deposits derived from the ranges. Source rock, fracture density, sediment production rate and transport process all influence the geomorphology, particle size distribution, and pedogenesis of surficial deposits. As the generation of hillslope sediment occurs through chemical and physical weathering of the underlying bedrock, discontinuity frequency and pervasiveness, such as joints or bedding within *in situ* bedrock, influence the relative availability of readily transportable sediment. Where the production of sediment exceeds the transport rate, hillslopes are mantled with colluvium, often grading into downslope alluvial surfaces. Mappable colluvial deposits and more organic-rich soils (Qha and Qmc within map on plate 1) are spatially restricted to higher elevations with greater precipitation and biogenic activity (fig. 5). As depicted in figure 5, hillslope materials exhibit considerable variability in age and extent and therefore cannot be represented effectively at the scale of mapping. Some larger Qha deposits are shown on the map on plate 1, but these polygons are not representative of the actual distribution of deposits because evidence cannot be obtained solely from remote sensing. Even so, hillslope deposits (Qha and Qhs) comprise over 39% of the map surface area.

Regional changes in climate or localized changes in the base level arising from tectonics are likely triggers to alter the relative amount of sediment production, transport process, and storage on hillslopes. Under the present arid climate, for instance, weathering rates are thought to be low and larger deposits of Holocene-aged slope deposits are relatively rare. In contrast, Pleistocene-aged deposits were generated under wetter glacial/pluvial climatic episodes presumably accompanied by higher weathering rates (e.g., Forester and others, 1999). Darkly varnished relict colluvial boulder deposits, observed throughout the map area, are particularly conspicuous on the volcanic rocks of the McCullough Range. Whitney and Harrington (1993) noted similar highly varnished deposits within volcanic rocks in the Yucca Mountain region, inferring that optimal boulder-forming conditions did not exist during late Pleistocene to Holocene time. Rock varnish, a manganiferous dark coating common on rocks in arid landscapes, is distinct from the underlying rock and is largely delivered from the atmosphere by precipitation, aerosols, dust, and dew (Liu and Broecker, 2000). Although rock varnish can form on virtually all rock types, its growth rate appears to be related to rock type. Carbonate and intrusive felsic volcanic rocks, for instance, express less varnish accumulation than extrusive mafic volcanic rocks. Although growth rates vary greatly and rock varnish does not directly correlate with age of associated geomorphic feature (Liu and Broecker, 2000), it does provide a relative age indicator when viewed at the scale of mappable geologic units.

Variability in weathering rates and products between different rock types also influences surficial deposits. Plutonic rocks, for example, were emplaced at deep depths and tend to produce homogeneous mineralogic assemblages. Once exposed at the surface, plutonic rocks tend to weather along mineral boundaries such that the granular constituents are relatively equal-sized (coarse sand and fine gravel), individual minerals available for transport. This degenerated granite, or grus, effectively is pre-sorted with respect to grain size at the outcrop. The resulting alluvial deposits have similar grain size distributions from the mountain front to the valley axis

(fig. 6). That is, comminution of particles with subsequent transport down the fan does little to change the overall particle size distribution. Within the map area, the gneissic Early Proterozoic granitoids and associated pegmatitic dikes (largely units mr+fpg, fpg+mr in the map on plate 1) are the most widespread producers of grus-like alluvium. These rocks, present in the Lucy Gray, southern McCullough, and southeastern Clark Mountain Ranges, are derived from a combination of plutonic emplacement and subsequent metamorphism. This source rock produces semi-grussy alluvium with a semi-uniform grain size distribution. Similar parent materials are the meta-igneous rocks (mr) located at the north end of the Mesquite Mountains and northeastern Kingston Range. The sole isolated Cretaceous pluton (Qpi-fp on southwest corner of map on plate 1) is limited in spatial extent and insignificantly alters alluvial deposit texture. The late Tertiary granite of the Kingston Range has an even shorter tectonic history and consequently lower fracture density and less granular disintegration and hence little grus is available for transport. Granular weathering of this young granite (~12.4 Ma, Fowler and Calzia, 1999) is considerably less than Cretaceous granitic and gneissic Precambrian rocks that are commonly granular at the outcrop. The local exfoliation and granular weathering of the resistant Tertiary granite in Beck Canyon within the Kingston Range appears to be related to northwest slope aspect and relatively high elevation.

In a parallel study of the Tertiary Kingston Peak Formation granite, Schmidt and Menges (2003) examined time-dependent characteristics, such as relative rock hardness of *in situ* bedrock and alluvial clasts. Rock hardness, as represented by type-L Schmidt Hammer measurements, was defined as a proxy for relative weathering with a minimum of 100 measurements on boulders of a given age deposit or on *in situ* bedrock with different exposure histories. Relative exposure age of bedrock was determined from the degree of desert varnish maturity using a Munsell® color chart for soils. Unvarnished rock, assumed to have a Holocene exposure age, had a Munsell® color of light bluish gray (Gley 2 8/5PB) (fig. 7), while varnished rock, assumed to have a Pleistocene exposure age, had a darker color of reddish black (2.5YR 2.5/1). In their study of debris-flow deposits, Schmidt and Menges (2003) report that rock strength is highest for Holocene-aged boulders and decreases for Pleistocene-aged material as boulders weather to grus. Similarly, figure 8 depicts the relative decrease in rock hardness from median Schmidt Hammer values of 53 for bedrock exposures that are relatively unweathered, to a median value of 37 for rock weathering to grus. This decrease in surface hardness is thought to be a function of weathering, as intact rock surfaces convert to granular mineral assemblages of grus.

Transport processes conveying sediment from bedrock uplands to piedmonts and channels can be broadly categorized into overland flow, fluvial, and mass wasting (debris flow) mechanisms. Overland flow occurs where infiltration capacities are low and water flow is unchanneled. Alluvial channels within bedrock source areas are typically single-thread and confined by bedrock valley walls. Although sediment transported through channels is conveyed predominantly through fluvial processes, steep hillslopes within the Spring and Kingston Ranges, for example, exhibit deposits formed from a combination of fluvial and debris-flow-dominated alluvial fans along the range front.

Post-depositional pedogenesis is influenced by both chemical composition and particle-size distribution. For instance, clast weathering within surficial deposits serves to modify deposit characteristics such that dissolution of carbonate clasts may enhance rates of pedogenic carbonate

formation. Fan deposits derived from carbonate parent material appear to produce more advanced pedogenic petrocalcic (B_{km}) and calcic illuviation (B_{tk}) horizons compared to non-carbonate parent material. Similarly, gypsum from late Paleozoic units on the west slope of the Spring Mountains is the likely source of the gypsum crystals in groundwater discharge and playa deposits in Mesquite Valley and southern Pahrump Valley. Alluvium composed of grus is generally associated with less pronounced bar and swale topography at the surface, weak to absent pavements, and less sorting and structure to the stratigraphy. The relatively narrow particle size distribution common to grus likely provides less opportunity to form a desert pavement through segregation of grain sizes by kinetic sieving and the progressive input of fine-grained eolian material. Particle texture influences the rate and depth of leaching such that the leaching depth is greater for coarse gravel. Counteracting the effective leaching depth, though, is the availability of fine-grained material. For the same duration of pedogenesis, an argillic horizon could form in a deposit with a fine-textured parent material but not in a sandy material, such as grus, because illuviation is a translocation function of the original fine-grained material. Devoid of a well-developed pavement and A_v horizon, grus-rich deposits are more prone to subsequent reworking of deposits, and pedogenesis is less developed for an equivalent aged deposit composed of non-granitic material. For example, the most advanced soil observed within middle Pleistocene grussy units is an argillic horizon, not a petrocalcic horizon as would be common for such an aged deposit composed of non-grussy parent material. The homogeneous texture, absence of desert pavement, and immature pedogenic development all contribute to grussy deposits that are readily remobilized by water and bioturbation.

Alluvial processes

In much of the map area, bedrock ranges are flanked by piedmonts composed of alluvial fan and axial valley drainage deposits including varying amounts of eolian sediment. Alluvial fans form where higher gradient, single-thread channels exit the confinement of bedrock source areas and sediment and water discharge into intermontane basins. The abrupt widening and channel cross-section shoaling at mountain fronts leads to a loss of competence, anastomosing channels, and sheet-like, parallel stratification. Fan morphology ranges from relatively symmetric, isolated aggradational fans such as those east of Ivanpah Lake emanating from the Lucy Gray Mountains, to those on the slopes of the Spring Mountains that coalesced into a continuous piedmont bordering the range. Alternatively, some disaggregated alluvial fans occupy long-lived deeply embayed valleys in mountain fronts, for example, i) Goodsprings Valley formed by tectonics, ii) the hourglass shaped fan draining from the McCullough Range through the Lucy Gray Mountains to form a symmetrical fan, or iii) the linear valley draining the east side of the Kingston Range. Axial valley drainages separate distal alluvial fan deposits sourced from opposite sides of a valley with flow and sediment transport occurring at roughly orthogonal directions to the alluvial fan deposits. Flowing longer distances than the neighboring alluvial fans, axial valley drainages occupy topographically low areas of a valley and integrate numerous source areas. Representative examples of axial valley deposits are located in Ivanpah and Shadow Valleys.

Alluvial fan deposits, in general, share similar sedimentologic properties such that they are poorly to moderately sorted, massive to well bedded, and clast- to matrix-supported. Sedimentologic differences arise in conjunction with depositional process. Sediment transport,

occurring dominantly by Newtonian, gravity-driven, channelized, fluvial flow and sheetflow, produces deposits of sandy gravel with local accumulations of cobbles or fine-grained lenses of gravely sand and sand. Fluvial facies include coarse-grained channel bars separated by finer grained swales. Depositional bars are characterized by non-indurated gravel, cobble, and boulder clasts with variable imbrication. Swale deposits include fine-grained, silt-rich, sandy gravel and gravely sand. The local grain size of these two facies is somewhat dependent on the position on the fan network and the bedrock and alluvial sources for the fan deposits. In proximal alluvial fans, the grain size tends to be greater because larger material was available for transport and streamflow generated from the bedrock uplands concentrates in the single-thread deep channels. The distal fan reaches, in contrast, tend to be finer grained where braided or anastomosing channels typically have shallow depths and lower sediment transport capacities. Preliminary field observations indicate that active channel gradients also decrease in distal reaches where surface sand fractions increase (Stock and others, 2004). Isolated large clasts, though, are commonly located in distal fan segments and their relative mobility may be enhanced by the increase in surface sand fraction by either altering boundary shear stress configurations or relative velocities necessary to entrain sediment. Distal fan deposits are composed of largely reworked sediments from intra-fan drainages. Valley axis deposits are typically coarse sand and generally finer-grained than neighboring distal fan material and may include deposits originating from groundwater discharge and eolian process. Valley axis floodplains are located in Ivanpah, southern Pahrump, Shadow, and the northern end of Mesquite Valleys. In southern Pahrump Valley, a road network constructed in the late 1960's has partially redirected the active channels.

Locally non-Newtonian, viscous slurry, granular, debris flows and hyperconcentrated flows deposit just downslope of mountain fronts or tributary junctions. Although not systematically mapped due to field constraints, the map on plate 1 depicts debris-flow deposits where fan gradients are high to moderate surrounding the Kingston Range, in the canyon west of Beer Bottle Pass, and north of Goodsprings, Nevada. Massive debris-flow deposits are commonly composed of a matrix of fine-grained material, typically sandy, fine gravel, with randomly orientated, rounded to angular clasts up to meters in diameter. Observed matrix material displays variable consistency. These high-sediment-concentration debris-flow deposits are preserved in fans with rugged topography and relatively steep slopes ($>5^\circ$). Deposits are massive, matrix-supported to poorly sorted without internal sedimentary structures but locally imbricated at the snout or along the levees. Surface morphology is characterized by lateral levees bounding the channels and coarse, steep-fronted, terminal lobes. In the Kingston Range, the granitic deposits have isolated boulders as large as 7 m in diameter resembling glacial erratics and precariously balanced boulders meters above the active channel (fig. 9). Younger, smaller volume fluvial deposits are generally confined to channel axes in debris-flow dominated proximal fans (fig. 6). Although debris-flow deposits were also observed in distal fans, they are relatively uncommon and are composed of smaller grain sizes. Although rare, debris-flow deposits in distal fans indicate either that debris flows arise from the intra-fan drainages or that debris flows originating in bedrock uplands travel long distances traversing much of the entire fan.

Schmidt and Menges (2003) estimated watershed-scale, debris-flow erosion rates in the Kingston Range through a combination of field studies and geographic information system (GIS) analyses. Ages of debris-flow deposits were determined in the field by their topographic and stratigraphic position, soil development, vegetation assemblages, boulder characteristics,

entrained historic material, and by prior dating with infrared stimulated luminescence (IRSL). Schmidt and Menges (2003) report that debris-flow depositional sequences from the steep, granitic hillslopes of the Kingston Range, are commensurate in age with nearby fluvial deposits. Volumes of age-stratified debris-flow deposits, constrained by deposit thickness above bedrock, GPS surveys, and geologic mapping, are greatest for Pleistocene deposits. Shallow landslide susceptibility, derived from a topographically based GIS model, in conjunction with deposit volumes produces watershed-scale erosion rates of $\sim 2\text{--}47 \text{ mm ka}^{-1}$, with time-averaged Holocene rates exceeding Pleistocene rates.

Within a separate fan or piedmont, the succession of progressively older alluvial units typically corresponds with topographically higher and more crowned deposits with advanced stages of pedogenesis (see Introduction section for additional pedogenesis discussion). The classification used here to separate alluvial deposits, based largely on Yount and others (1994), has four main time-based divisions: old (OA), intermediate (IA), young (YA), and active (AA) alluvial fan deposits. Combined these four units comprise almost half (48%) of the map area. Deposits derived from other geomorphic processes are classified using the same divisions. Deposits classified as old alluvial fan deposits (OA) form ballenas or linear ridges that resemble breaching whalebacks with distinctly rounded lateral margins located at varying heights (up to many meters) above the active channels (Peterson, 1981). These Qoa deposits comprise about 9% of the map planform area. The crowned profile of these deposits reflects the efficacy of surface erosion in removing the upper soil horizons, occasionally leaving a lag of coarse alluvial clasts and pedogenic calcic fragments on the surface (fig. 10). Soil horizons remaining on the deposits are usually well developed with stage IV (Gile and others, 1966) or higher petrocalcic horizons (Machette, 1985) (fig. 11), and occasional thin, degraded argillic horizons (Yount and others, 1994). Because petrocalcic material is present at the surface, these features often appear light in color with high albedos on DOQQ's and tend to be located in proximal fan environments near the bedrock to alluvial contact. The 0.74 Ma Bishop ash is the most diagnostic tephra layer observed regionally in OA deposits (McDonald, 1994). Although active urbanization along the northern map boundary made many unit calls difficult, the extensive OA-aged deposits at the northern end of the McCullough Range, however, express characteristic high-relief profiles and advanced petrocalcic B_{km} horizons with calcium carbonate stage IV development. Although deposit surfaces have been anthropogenically modified, the overall morphology is quite characteristic and hence the unit calls have a high confidence and the dissected Qoa units occupy most of the area.

Intermediate age (IA) alluvial fan deposits, comprising about 16% of the map area, display a characteristic desert pavement with interlocking surface clasts (fig. 12) overlying a vesicular A_v horizon, or A_v . Pavement surfaces, typically one clast thick, consist of particle sizes ranging from gravel to boulder that are variably varnished depending on source rock type. Older surfaces of IA-age tend to display A_v horizons with well-developed vesicles, silt-dominated texture, and platy structures arising from relatively well-developed ped faces. Younger IA-aged surfaces display more sand-rich A_v horizons and poorly developed ped faces. Varying amounts of red to brown clay accumulation and iron oxidation alter the B-horizon soil color (B_w to B_t horizon). Stage I to III B_{km} horizon development is also common, and is expressed as calcium carbonate coatings, rinds, nodules and accumulations between clasts (Gile and others, 1966; Machette, 1985) (fig. 13). Deposits of IA-age appear dark toned (low albedo) on aerial photography and DOQQ's from the presence of rock varnish and lack of vegetation (fig. 14), and are found more commonly in

proximal fan positions. Although also located in medial and distal environments, they tend to decrease in abundance with distance from mountain fronts either because of subsequent erosional reworking or by burial. Planform profiles appear as stranded, elongate to diamond shaped, landforms reflecting the pattern of fan incision. The vertical separation between deposit surfaces and differences in gradient with respect to younger inset surfaces vary with timing of incision and the relative age of the deposit. Most surfaces retaining desert pavements have been dated as late Pleistocene, with some falling in the range of late-middle Pleistocene age range (Bull, 1991).

Young alluvial (YA) fan deposits, the largest alluvial unit mapped comprising 22% of the area, typically consist of sand- and gravel-sized material with well- to moderately-developed bar and swale topography and immature pedogenesis (fig. 15). Bars are coarser grained than swales. Where present, soil development is restricted to the oldest surfaces, and consists of an incipient A_v horizon overlying an incipient B_w (cambic horizon). Calcic development is limited to stage I to II. Young units are typically light-toned on aerial photography, with varying amounts of tonal changes due to source lithology, inherited rock varnish from remobilized material, and vegetation density. Deposits with dense cryptobiotic soil crusts appear darker toned on aerial photography. Biotic soil crusts are common and can form thick mats or 'carpets' dominated by lichens, particularly on sediments derived from granitic source material. Deposits of YA-age are moderately vegetated with creosote, ambrosia and annual grasses. The YA deposits are typically present throughout the alluvial fan environment and are the most aerially widespread surficial deposit in the map area. Source material for YA-aged deposits can be quite varied, including the reworking of previously deposited alluvium. For example, in Hidden Valley a degraded OA-aged deposit is presently eroding to produce YA-aged deposit composed predominantly of petrocalcic fragments derived from an exposed and eroding B_{km} horizon. Age data collected on YA deposits range from latest Pleistocene through modern.

Active alluvial (AA) deposits, comprising <3% of the map area, consist largely of narrow gravelly to sandy bars or terraces surrounding active alluvial channels and are typically inset along the margins of YA deposits (fig. 16). Bar and swale topography is pronounced and largely reflects original depositional morphology. The deposit surfaces lack desert pavements and rock varnish. Pedogenic development, present only in older units of this time period, is limited to fine sand and silt accumulations in the upper 10 cm, but may also be attributed to overbank deposition of fine sediment during floods from active channels devoid of pedogenesis. Active alluvium tends to be light gray in color and is comparatively loose without appreciable cohesion that cannot retain a vertical face when excavated under dry conditions. Mappable AA-aged deposits, present across the entire fan environment, are concentrated adjacent to larger active channels. Active channels are largely unvegetated, even by annual grasses. On aerial photography the active channels and associated terraces tend to be light toned to white (high albedo), elongate in the down-fan direction with narrow aspect ratios and have rough microtopography. Although ages of older AA deposits are uncertain, evidence for minimum ages of these deposits exists in the form of burial or erosion of dateable anthropogenic impacts. Burial or degradation of anthropogenic features, such as stripping or burial of roads, tin cans, glass, and equipment often associated with mining or military operations provide relative dating and inferences can be made regarding the magnitude, timing and frequency of alluvial activity. The younger active units (dominantly channelized) often bury or erode recently graded roads. Many of these events are anecdotally attributed with El Niño generated or local convective storms. Frequency of sediment movement

within AA-aged channels leads to the interpretation that they are typically deposited on decadal or shorter time intervals. Even under the presently arid conditions, alluvial fans in the Southwest stochastically flood and aggrade (e.g., Field & Pearthree, 1997).

Active channels inset within older alluvial deposits can be incised up to several meters deep with steep colluvial deposits or eroded banks (fig. 17). Channel bottoms are mostly covered with active alluvium with neighboring terraces composed of alluvium older than the channel deposits. In the Spring Mountains, Lattman and Simonberg (1971) and in the McCullough Range, Lattman (1973) noted that less consolidated layers beneath the channel bed surface may undergo a case-hardening as water infiltration and weathering of exposed surfaces produces a carbonate layer penetrating to 50 cm thick on vertical and horizontal faces in as little as few months. This phenomenon known as the “wash effect” can partially stabilize the channel slowing lateral migration and subsequent vertical incision.

Eolian processes

Availability of airborne sediment is regulated by atmospheric conditions driving wind speed, the proximity to sources of fine-grained material, topographic constraints on local wind patterns, vegetation assemblages, and the magnitude of anthropogenic disturbance. Although eolian deposits, including sand sheets, dunes, and vegetation mounds, are well developed on the eastern and southeastern edges of valley axis and playa deposits throughout the map area, they comprise only 3.5% of the total planform map area. Locally extensive eolian deposits surrounding playas demonstrate the regional importance of eolian processes mobilizing sediment from local sources. For instance, sand dunes and ramps were mapped in Mesquite Lake, southern Pahrump Valley, Ivanpah, and Roach Lake Valleys (figs. 18 and 19); all locations adjacent to playas. Distal fans also may include significant eolian deposits depending on the prevailing wind direction and the availability of fine sediment from the distal fan and adjacent valley floor deposits. Deposits of eolian sediment commonly lap on to and stratify with deposits transported by alluvial and hillslope processes creating mixed genesis units. Eolian deposits, for instance, commonly grade into the distal alluvial fan deposits as sand sheets with vegetation mounds and small dunes that decrease in size and abundance up slope. In many distal fan zones, sand is concentrated along low gradient channels and channel filling dunes may overly inactive channels and vegetation.

Eolian deposits are actively remobilized from units with little or no vegetation, for example along dirt roads, and areas with low soil moisture whereas they are comparatively immobile where stabilized by abundant vegetation. Small accumulations of airborne transported silt and sand are also incorporated into vegetation mounds, commonly surrounding creosote bushes, or local sand sheets that spread over terraces between recently active channels. In southern portions of Pahrump and Mesquite Valleys, for example, vegetation-stabilized dunes and sand sheets are mixed with alluvium and the active sand transport appears to be locally derived by remobilization of older valley sediments uplifted along the Pahrump Valley fault zone and from the Mesquite Lake playa. Along the edge of Mesquite Lake are late Pleistocene wet playa deposits, including gypsum-rich sand, that have been stripped by wind erosion to produce erosional yardangs and deposited locally on the adjacent dunes and distal fan deposits to the southeast (figs. 20 and 21). Holocene and active sand deposits apparently reflect the potential on-

going deflation of groundwater discharge deposits in the southeast Mesquite Lake Valley. Similarly, north of Kingston Wash, superimposed sand deposits record long-lived, from the Quaternary to the early Holocene, regional-scale orographic influences that continue to affect active sand distribution. Similarly, Lundstrom and others (2003) report late Holocene ages for similar dunes in an adjoining part of the Las Vegas 30'X60' quadrangle.

Groundwater processes

The valley domain encompasses a range of depositional systems where fine-grained sediments typically accumulate to form playas that may provide local recharge but also denote areas of groundwater discharge. Water balance is key to interpreting playa characteristics such that all sources of precipitation, surface-water flow, and groundwater flow exceed evaporation and evapotranspiration. The flatness of playa surfaces likely results from deflation that erodes sediment down to the capillary fringe where higher water contents serve to decrease relative erodibility. Playa flatness also arises from the deposition of clastic material through widespread, low-energy flooding. Playa deposits are subdivided into dry and wet playas following terminology proposed by Langer and Kerr (1966), Rosen (1994), and Briere (2000). As discussed in Langer and Kerr (1966), dry playa deposits are formed by the ponding of ephemeral surface water on what is commonly called a dry lake bed (fig. 22). Dry playas are recharging basins occur where water tables are sufficiently deep such that capillary zones do not affect the surface that can be hard packed, smooth, and dry (fig. 23). Dry playas do not accumulate saline minerals such that a runoff-fed lake is too short-lived to precipitate evaporate minerals. Ivanpah and Roach Lake playas are typical dry playas where abundance of clays transported by surface runoff proves to be the factor controlling surface morphology of the impervious basin floor with low recharge and high evaporation rates. A small active dry playa also lies in the low part of a wind-deflated basin in southern Mesquite Valley. The surface of dry playas is typically barren and compact in the dry season, though it may be muddy and covered with standing water for days after seasonal rains. Langer (1965) noted that extensive desiccation cracks occur in playa sediments with 50% or more clay such that polygonal fractures are common in the desiccating fine-grained sediment.

Wet playas are discharging intracontinental basins with a negative water balance, remaining dry 75% of the year, often associated with evaporite minerals (Rosen, 1994; Briere, 2000). At Franklin Playa on the Amargosa River within the neighboring Death Valley quadrangle, for instance, Czarnecki (1990) measured groundwater discharge rates of 1 to 4 m³/day in areas of active deposition during the summer months. The term wet or discharging playa describes fine-grained deposits where groundwater discharge is an important factor governing the morphology of the valley deposits. The capillary fringe is sufficiently close to the surface such that evaporation causes water to discharge, resulting in precipitation of evaporite minerals. Evapotranspiration induces the precipitation of soluble minerals in the upper soil horizons and deposits below (Rosen, 1994). Evaporites tend to form only in intermediate periods of wetness when evaporation is high and water input is balanced by evaporation. If conditions are overly wet, the water is too fresh for brines to develop. Similarly, for significant accumulations of gypsum to form, there must be a high proportion of groundwater entering the lake and ample sources of calcium from carbonate bedrock. Active playa sediments composed of crystalline gypsum mixed with mud are shown in the map on plate 1 as wet playa deposits (Qapw) and figure 24. Rosen (1994) notes that displacive crystals, intergrown within the playa matrix, form by

precipitation of interstitial brines where groundwater discharges by evapotranspiration. In Mesquite Valley, eolian deflation of late Pleistocene deposits has exposed a more stable substrate of mud and crystalline gypsum, mixed in layers up to one meter thick (fig. 25). At the southeast end of the Mesquite Valley, gypsum sand eroded from the playa deposits on the valley floor have been redeposited as YA to AA-aged gypsiferous dunes.

In Mesquite Valley, groundwater discharge by evapotranspiration has produced a wet playa with a characteristic soft, low density, inflated surface. Langer (1965) attributed the puffy texture to a clay-water-salt interaction combining to produce a “self-rising soil.” Much of the ground in Mesquite Valley is marked by soft porous silt and clay to a depth a few tens of centimeters. This soft porous soil is commonly covered by a crust, approximately 1 cm thick, that is weakly cemented by salts and clays. Cementation by salts, largely gypsum, increases below 10 to 15 cm (fig. 26). Anthropogenically disturbed areas, where the somewhat fragile crust has been broken, have the potential to produce silt-sized sediment for wind transport in proportion to the surface area of the disturbance. The extent of active wet playa deposits in Mesquite Valley is difficult to ascertain because the boundaries of the saturated zone undoubtedly varies from season to season. In the southern part of Mesquite Valley, Late Pleistocene wet playa deposits are clearly inactive where the surface has been stripped by wind erosion and incised channels contain early to mid Holocene gravels.

Notable groundwater discharge deposits are located adjacent to the distal fans of southwest Mesquite Lake. This includes an active groundwater discharge zone at the base of the fan east of Mesquite Pass and late Holocene zone on the adjacent fan to north. Active groundwater discharge was recognized by the presence of mesquite and catclaw and local differences in the creosote vigor. Notably the creosote brush in the active discharge zones is up to 0.5 m taller than on adjacent alluvial fan surfaces. At the time of the field observations (November, 2003), creosote bushes in the discharge zone were thickly foliated with green, flexible branches, while creosote on the strictly alluvial surfaces was dry with brownish green foliage and brittle branches. Groundwater discharge was also marked by a red-brown, declining population of phreatophytes and invasive salt tolerate plant species; notably saltbushes (*Atriplex*). The vegetation indicative of declining vigor probably marks a combination of decreased recharge on the fan and incursion of alkaline waters from Mesquite Lake Valley progressing from the late Pleistocene to the present. Groundwater discharge may also result in deposition of shallow carbonate, amorphous silica, and gypsum concentrations.

An active zone of groundwater discharge at the playa fringe (Qypf in map on plate 1) was also observed west of Black Butte at the foot of the fans from the northeast Kingston Range and at the foot of fans from the east slope of the Mesquite Mountains. In the northeast Kingston Range, groundwater discharge at the toe of the fan is marked by a stand of healthy creosote and grasses expressing notably higher density and better health than surrounding areas. Creosote over 2 m in height were noteworthy because of their vibrant-green robust growth compared to creosote outside of the groundwater discharge zone with a brownish-tinge. North of the Mesquite Lake playa, groundwater discharge is indicated by an extensive stand of mesquite along the distal part of the fan from Winters Pass. Distal-fan groundwater discharge deposits are also included in the playa fringe deposits on the west side of the Mesquite Lake playa at the base of the alluvial fan from the Mesquite Pass area.

Where shallow groundwater or springs support moderately dense vegetation, fine-grained sediments can be trapped to form extensive sand sheet and vegetation for a fringe zone at the toe of fans. Quade and others (1995) referred to such zones as phreatophyte flats in the distal fan zone. The result is a mixed unit of eolian and alluvial sediment controlled by the distribution of vegetation and commonly reshaped by bioturbation. In the map on plate 1, phreatophyte flats are included in the playa fringe unit (i.e., Qypf), typically including mixed eolian and braided stream deposits. This unit is distinguished on aerial photographs and in the field by the abundance of phreatophytes such as mesquite and acacia or zones of extraordinarily robust examples of xerophytes such as creosote. Quade and others (1995) suggested that inactive discharge deposits, including those near Stump Spring and in the Sandy Valley area, are evidence of declining shallow groundwater in response to short-term climate change. Older Quaternary deposits (Qov) exposed beneath late Pleistocene groundwater discharge deposits at Stump Spring (Qig) contain evidence of paleo-discharge events. The older section, however, is folded and faulted and includes sediments from valley axis deposits (Qov) that include cross-bedded eolian and fluvial sand beds and paleosols.

Present rates of groundwater recharge within the study area are likely extremely low and highly localized to playas or larger wash systems with thick sections of permeable sediments. As small intra-fan washes are typically inset into older units with potentially well-developed pedogenic horizons, most soil moisture derived from precipitation interfaces at shallow depths with low conductivity layers that likely retard significant groundwater recharge. Even under the current arid climatic conditions, however, small amounts of recharge occur as infiltration of intermittent runoff in larger washes (Izbicki and others, 2000). On the basis of tritium-based tracer studies, Izbicki and others (2000) concluded that the average rate of water movement is 0.7 m/year in the Oro Grande Wash near Victorville, California. As this rate is rather slow, any connectivity between climatic induced variations in streamflow and groundwater tables would be temporally dampened.

Lattman (1973, 1977) described the case-hardening effect of pedogenic calcium carbonate produced by infiltration of water within older alluvial deposits in a study on the northwest slope of the volcanic McCullough Range. He hypothesized that mechanical weathering of caliche deposits on Qoa deposits produces a layer of coarse rubble, protecting the remaining underlying carbonate layer from weathering. Lattman (1973, 1977) asserted these low angle layers, forming within the upper meter of deposits, are relatively impervious to water erosion and lateral migration of channels in the present arid climate, and hence the resistant caliche may preserve many older units within the modern landscape. He speculated that within older deposits, the poorly consolidated material above the carbonate layer is commonly removed by erosion leaving the resistant, tightly-cemented surface conglomerate and carbonate cement acts as a cap rock over less consolidated alluvium. These carbonate layers may be relatively impervious to water and thereby limit vertical infiltration of precipitation and favor runoff, hence shunting any groundwater recharge to downslope portions of the landscape.

Biologic processes

In this dryland landscape, ecosystem assemblages at the local scale are primarily modulated by available soil moisture and soil fertility. As soil moisture and fertility generally increase with elevation as precipitation is enhanced, surficial geologic units at higher elevations typically contain greater amounts of organic materials incorporated into the soils and more frequent bioturbation disrupts soil horizonation. At lower elevations, the creosote bush, an evergreen xerophytic perennial shrub, is one of the most common plants throughout the piedmonts and valley floors. Although currently quite ubiquitous, creosote bush was one of the slower immigrants into the Mojave Desert through the Holocene (Spaulding, 1990; Koehler and others, 2005). The relative success of the creosote bush under the current climatic conditions of sporadic precipitation, extended periods of low soil moisture, low soil fertility, high solar radiation, and high air temperatures stems from its ability to adjust vegetative and reproductive growth patterns in response to environmental changes (Sharifi and others, 1988). Although water is generally the most important variable influencing productivity and resource allocation, during extended durations of abundant soil moisture that promotes growth, available nitrogen is the likely factor that limits productivity of desert ecosystems. For instance, Cunningham and others (1979) and Sharifi and others (1988) reported that soil moisture alone cannot be used to predict creosote productivity such that nitrogen availability also limits growth.

As nitrogen is leached from soils to support vascular plants, the importance of biologic soil crusts is paramount to sustaining desert ecosystems (NRCS, 1997). Biologic soil crusts, communities of cyanobacteria, lichen, and mosses, increase physical soil stability and influence vascular plant germination and success primarily through nitrogen fixation (Johansen, 1993) (fig. 27). In addition to stimulating plant biomass through fixing nitrogen, soil crusts physically stabilize soil and thereby reduce fluvial and eolian erosion and physical disturbance, roughen ground surface microtopography, retain moisture, and trap seeds. The presence and density of biological soil crusts provides a relative measure of surface age given that lichen and moss colonization requires long-term surface stability. *Collema* lichen, for instance, may require a stable surface for as long as 1000 years post disturbance in order to successfully colonize (J. Belnap, personal communication, 2002). As there is an inherent link between deposit age and biologic crust assemblages, surficial geologic maps may be used as a template to predict and extrapolate the presence of biologic soil crusts. In addition, the redistribution of water within the soil through surface rainfall/runoff patterns may significantly influence hydrologic and biologic processes. Spatially variable infiltration capacities modified by the presence of soil crusts and pedogenic maturity may provide a connection between rainfall, runoff, soil moisture, and vegetation vigor and density.

Relations between surficial deposits and the associated biologic processes operating on them are temporally variable as floral and faunal assemblages in the map area varied in response to climate change. For instance, macrofossils preserved in packrat middens document the expansion of dryland vegetation following the last glacial maximum and the restriction of woodlands to isolated highlands with higher precipitation and lower temperatures (e.g., Koehler and others, 2005). Constraints from packrat middens also indicate that the present Mojave Desert flora existed in its current general form during only the last ~10,000 yrs (Spaulding, 1990). Deglacial climate change (~12,000 to 10,000 yr B.P.) led to regional northward migration of numerous plants, but biotic changes tend to be time-transgressive and likely vary with local site

conditions such that Koehler and others (2005) concluded from packrat middens that the region between 35° and 37° N latitude marked the boundary between milder, moister environments to the south and colder, drier environments to the north.

Quaternary Tectonics

Although numerous Pre-Quaternary faults were mapped in the region by offset bedrock exposures (e.g., Hewett, 1956), few Quaternary faults besides the Pahrump Valley/Stateline fault zone were previously recognized. Bedrock geology records pre-Quaternary tectonic deformation dating from Proterozoic basin formation, through late Paleozoic to Mesozoic crustal shortening, culminating in mid Tertiary crustal extension (e.g., Hewett, 1956; Jennings and others, 1962; Longwell and others, 1965; Wright, 1968; Burchfiel and others, 1974; Calzia and others, 2000). Hewett (1956) portrayed numerous pre-Quaternary faults within bedrock, in addition to a few projecting through Quaternary alluvium including: i) the McCullough fault traversing the valley separating the Lucy Gray and McCullough Ranges, ii) the Sheep Mountain fault, splaying from the McCullough fault, to the northwest and separating the eastern edge of the Lucy Gray Range from Sheep Mountain, iii) the Roach fault to the west of Roach Lake, iv) the State Line fault extending from the southern Spring Mountains to the southern tip of the Lucy Gray Range, and v) numerous northwesterly trending faults in the Bird Spring Range. Previous studies did not identify many Quaternary tectonic structures, in part, because the active faults have little similarity to older bedrock structures. Conversely, it is difficult to distinguish bedrock structures that might have been active in the Quaternary because of the scarcity of Quaternary deposits to preserve records of recent movements. Strike-slip faults described by Hewett (1956), Clary (1967), McMackin (1992) and Prave and McMackin (1999) are aligned with some of the active Quaternary structures described in this report.

Newly mapped Quaternary faults presented in the map on plate 1, table 1, and figure 28 are located in Pahrump and Shadow Valleys, the Bird Spring, Lucy Gray, Highland, and Kingston Ranges as well in Kingston Wash. Faults and folds observed in Quaternary deposits cut early to late Pleistocene (Qox and Qix) deposits and are commonly overlain by late Pleistocene and Holocene deposits providing stratigraphic limits on the age of most recent activity. No strictly Holocene ruptures were identified either from remote sensing or field observations. Fault orientations are varied with strikes primarily north-northwesterly directed, but some strike northeast as well (fig. 28 and table 1). Landscape positions range from basin bounding at mountain fronts to valley bottoms and hence are not associated with any individual landscape features such as playas, axial valleys, or mountain fronts. Although normal faulting appears to be most prevalent, strike-slip offset with both dextral and sinistral senses of deformation were observed. One lineament was mapped in the center of Mesquite Lake Valley. Other tectonic features depicted in the map on plate 1 include faults and low-amplitude folding in localized zones of uplift and subsidence with pronounced stream incision resulting from tectonically induced base level changes. The subsequent discussion of tectonic features is presented in accordance with the labels depicted in fig. 28. None of the faults depicted here currently exist in the U.S. Geological Survey online database of Quaternary faults and folds (<http://earthquakes.usgs.gov/qfaults/nv/index.html>). All faults in the map on plate 1 correlate to fault class A of this online database (Class A definition: geologic evidence demonstrates the existence of a Quaternary fault of tectonic origin, whether the fault is exposed by mapping or inferred from

liquefaction or other deformational features). The lineament shown in the map on plate 1 correspond to class C such that the observed geologic evidence is insufficient to demonstrate (1) the existence of tectonic faulting, or (2) Quaternary slip or deformation associated with the feature.

Among the Quaternary faults in the map area, the southern extension of the Pahrump Valley and Stateline faults are the primary tectonic features and are the most commonly recognized (e.g., Hewett, 1956; Hoffard, 1991; Anderson and others, 1995; and Louie and others 1998), where multiple traces are broadly aligned in Pahrump and Mesquite Valleys along the California-Nevada state border (A, fig. 28). Louie and others (1998) referred to the combined Stewart Valley fault, Pahrump Valley fault, and Stateline faults as the Pahrump Valley fault zone (PVFZ), noting that the combined length of all three faults as a fault zone may exceed 100 km in length while Anderson and others (1995) estimate the system extends up to 130 km long. The southern portion of this zone extends from southern Pahrump Valley to Stateline Pass and contains features A, B, E, F, and J shown on figure 28. Anderson and others (1995) estimated the vertical slip rate on the southern Pahrump Valley fault near Stump Spring, but that measurement, based on fault scarp height, may have over-estimated the age of ground water discharge deposits and only accounted for vertical displacement. Quade and others (1995) estimated the age of the oldest groundwater discharge event to be $>450,000$ yr B.P. in southern Pahrump Valley. Subsequent age determinations by thermoluminescence, from older Quaternary units below the carbonate layer yielded ages between 275 ka and 400 ka (Lundstrom and others, 2003) revealing that the slip rate must be somewhat higher. Louie and others (1998) estimated that the dextral slip rate component on the Stewart Valley fault may be above 0.1 mm/yr.

McMackin (1999) reported that the PVFZ does not offset Qig carbonate deposits that drape a fault scarp, but suggested that later deformation was expressed as transpressional folding (A, fig. 28). The Qig carbonate deposits are deformed by systematically oriented neotectonic joints in folds. These joints constitute two main sets with one striking northeast, approximately perpendicular to the approximate fold axis and one northwest approximately parallel to axis of folding. Reorganization of late Pleistocene to Holocene patterns of incision and deposition in southern Pahrump Valley likely reflect uplift west of the fault associated with folding.

Two north-striking faults were observed in the mid-fan portion of Lovell Wash (B, fig. 28). The faults, clearly visible on DOQQ and Landsat7 imagery, include fault scarps and local changes in slope. Although the faults offset a denuded carbonate horizon within older alluvial deposits (Qoa), they are overlain by unfaulted late Pleistocene alluvial deposits (Qia). These faults are aligned with, and parallel to, a down-to-the-west normal fault on the west edge of pull-apart basin north of the Pahrump Valley fault in the northern part of Pahrump Valley (Hoffard, 1991; Lundstrom and others, 2003).

Although no conclusive tectonic offset of Quaternary deposits in the Bird Spring Range (C, fig. 28) were observed during this study, Hewett (1956) mapped numerous northwesterly striking faults. Features consistent with Quaternary tectonic deformation, however, were identified including linear relationships between i) topographic gradient breaks within alluvial deposits, ii) subtle changes in Quaternary units from steep ($\sim 15^\circ$) Qha/ca to lower gradient ($\sim 4^\circ$) Qoa/sl map units, iii) abruptly truncated Qoa deposits with broadly triangular facets at contacts

with Qia deposits (fig. 29), iv) groundwater deposits oriented along trend of map unit breaks, v) a trough in hillslope deposits and topographically back-facing Qha deposits (fig. 30), vi) a moderately linear trace and regional persistence of the above features, and lastly vii) a spatial correspondence of queried Quaternary faults with prominent bedrock shear zones of similar orientation. The northern extent of the queried faults in the Bird Spring Range corresponds with a topographic high in Qoa deposits such that the unit grades downslope in directions normal to the trend of the queried fault and fractures observed within Qoa deposit as well as highly disrupted ca and sl bedrock. Many features observed within Quaternary deposits, however, could be consistent with pre-Quaternary faulting such that subsequent deposits over-ride and mimic existing topography and hence the faults mapped in this region are labeled as queried features.

The single, almost north-trending, fault shown at the western edge of Qoa deposits in the north part of the Kingston Range (D, fig. 28), is indicated by an abruptly truncated Qoa ridge spurs. The late Pleistocene (Qia) and Holocene (Qya) terraces diverge downstream toward the scarp and return to common grade across the scarp, recording late Pleistocene to recent adjustment of the stream gradient. Maximum scarp height is approximately 5 m. The fault is oriented parallel to and aligned with bedrock faults bounding the northwest range-front in the Kingston Range (McMackin, 1992).

The presence of a major structural discontinuity within valley deposits of Pahrump Valley, sourced from the Spring Mountains, generates a feedback between tectonics and hydrology. In some areas along the Pahrump Valley fault zone, for instance, infiltration is concentrated along fractures in the carbonate layer resulting in piping as the water flows laterally beneath the cap rock. In the area near Stump Spring, such pipes provide a habitat for bats and other mammals. In the north end of Sandy Valley (E and F, fig. 28), Quade and others (1995) attributed groundwater discharge deposits, mapped here as Qig, to fault-controlled groundwater drainage.

Several northwest striking (G, fig. 28) and east-northeast striking parallel fault traces (H, fig. 28) cut older and intermediate Quaternary units on the piedmont south and southwest of Kingston Peak. Much of the potential exposure of these faults is concealed by recent eolian sand, largely eroded from older sandy units and re-deposited locally as active sand sheets and vegetation-stabilized dunes, but in many areas these faults can be recognized by eroded scarps or in exposures in fluvially dissected sections (fig. 31). Good exposures of some fault traces are found in dissected canyons that transect the piedmont. Although many fault strands exhibit vertical displacements across their scarps, largely right-lateral offset evidence is preserved within bedrock. Numerous fault traces of G and H are found in Qoa deposits, and while some traces cut the overlying Qia sediments, most are truncated at the base of Qia units (fig. 32). Carbonate-cemented Qoa sands preserve scarp morphology in several areas where vertical displacements produced prominent features.

McMackin (1992) described the Do Not Pass fault from exposures cutting late Proterozoic units that exhibit a minimum of 7 km of left-lateral slip. Field investigations for this study revealed significant offsets in older Quaternary deposits on trend with the fault in the north fork of Kingston Wash (I, fig. 28), southeast of Kingston Peak. In its only bedrock exposure, the fault occupies a zone approximately 0.5 km wide with intensely brecciated rock. Along the north fork of Kingston Wash, the fault has several exposed traces within Qoa deposits. Individual traces are

commonly braided with 1 to 2 m of offset and carbonate-coated fault surfaces. Although, none of the several fault surfaces inspected expressed slip indicators, the presence of north-trending fractures is consistent with left-lateral displacement; in agreement with McMackin (1992). The upper surface of the Qoa, an exposed B_k horizon, exhibits down to the northwest displacement of 20 to 30 m across the wash. Near the confluence of the north fork and main channel of Kingston Wash, Qoa sediments are folded and multiple fault traces are exposed in cut banks along the wash. A belt of older sandy deposits (Qoe and QToa) are offset approximately 7 km in left-lateral sense across the north Fork of Kingston Wash.

Within the Mesquite Lake playa, multiple sub-parallel lineament traces (J, fig. 28) separate the intermediate-aged crystal body playa deposits (Qipc) to the northeast from the active playa surface (Qap). These northwesterly trending lineaments are oriented parallel to and along strike with faults A and E and may represent a southeasterly extension of the PVFZ. The generalized mapped lineament was identified from subtle linear vegetation and tonal lineaments without clear tectonic offset and is associated with the Cub Lee well.

West of Shadow Mountain, two Quaternary faults (K, fig. 28) were observed in older alluvium (Qoa). These faults are aligned with faults in Tertiary bedrock exhibiting left-oblique slip. Northeast-trending aligned deposits of older alluvium (Qoa) indicate the approximate position of a buried east-northeast-striking fault (L) southeast of Shadow Mountain. This fault is parallel with an east-northeast trending fault in bedrock. Fault L is concealed by extensive intermediate (Qia) and younger (Qya) deposits eroded from Shadow Mountain to the north and west. The Qoa deposits in the area are distinctive because they contain clasts of granite from hills to the southeast in a source area that is no longer accessible by the active drainage network. These isolated gravel deposits from a southern source indicate a gradient reversal across the fault equivalent to several tens of meters displacement of older alluvial deposits (Qoa). The Quaternary age of the deposits is indicated by the surface morphology of the deposits and the moderate abundance of pedogenic carbonate chips in the pavements on the eroded surface.

Two faults displace older alluvial deposits in the valley between Clark Mountain and the Mesquite Mountains (M and N, fig. 28). On the north side of the valley, uplifted older alluvial deposits form truncated ridges along a range-bounding fault (N) on the south slope of the Mesquite Mountains. North-facing scarps up to 10 meters high in older alluvium (Qoa) of fault M are parallel to a bedrock shear zone at the south end of the adjacent bedrock hills.

A small queried fault is located east of Desert on the railroad corridor within Qia deposits (O, fig. 28) that corresponds with the southern extent of the Roach Fault mapped by Hewitt (1956). Fault O was inferred solely from irregular drainage patterns and tonal changes observed in remote sensing images without field checking and hence the feature may be a lineament. West of the Lucy Gray Mountains, Hewitt (1956) mapped the Roach fault, a normal fault that potentially connects with another northwest-striking fault, the Cottonwood fault, in the Bird Spring Range. Approximately 8 km northwest of and along strike with fault O lies a small outcrop of QToa, bounded by Qia deposits, on the west side of the Lucy Gray Mountains. This feature may be a fault-bounded expression of the Hewitt's Roach fault but no field evidence was observed to indicate a fault-bound relation. Either this QToa outcrop is a small erosional remnant buried by younger alluvium, or it represents a small block displaced by tectonic offset.

From a large-scale structural perspective, Hewett (1956) concluded that the McCullough fault, separating the Lucy Gray and McCullough Ranges, expresses about 6,096 m (20,000 feet) of normal displacement. Activity on this McCullough fault appears to have continued into the Quaternary as outcrops of Qha/mv truncate Qoag deposits (P, fig. 28). Along a north-northwest trend from these truncated Qoag deposits are Qygs deposits that likely arise from a fault-controlled disruption of groundwater flow but do not necessarily represented age constraints on the timing of most recent fault displacement. These spring deposits may also be related to the pediment margin within granitic material (Qpi-fpg).

In the southeast corner of the map, evidence for Quaternary deformation in the McCullough and Highland Ranges includes an east-west trending anticline, as well as a northwest-trending fault that juxtaposes Qoa and Qia outcrops (Q, fig. 28). Deeply incised Qia, Qoa, and QToa deposits in the headwaters to Piute Valley likely express changing base levels driven by local tectonic displacements associated with an east-west trending structural anticline through the Highland Spring Range, as recognized by Hewett (1956) and Longwell and others (1965). The presence of a long-lived east-west trending anticlinal structure is likely associated with the widespread exposures of QToa, the presence of a fault near the drainage divide to the Piute Valley system, and the highest relief within the McCullough Range at McCullough Mountain. The northwest-trending fault coincides with a 0.5 m topographic saddle between the mv dominated Qoa deposits and fp+mr dominated Qia deposits. The Qia deposits have a surface morphology characterized by moderate-relief linear ridges, while the Qoa deposit morphology is more diffused with broad, low-relief ridges. If the mv clasts within the Qoa deposits were sourced from the east in the Highland Range, the deposit surfaces should grade to the west. Rather, the Qoa deposits slope eastward, possibly representing a tectonically driven back-tilting of the valley floor.

Summary

The map presented here represents the first detailed surficial geologic map of the Mesquite Lake 30'X60' quadrangle. Alluvial units (Qaa, Qya, Qia, Qoa, and QToa) dominate, comprising roughly half of the map area with the spatially extensive Holocene alluvial deposits accounting for the bulk of Quaternary units. Undivided hillslope deposits mantling bedrock account for nearly 40% of the landscape. Units considered to show evidence of active erosion and deposition on the scale of years to decades (i.e., Qaa, Qaw, Qae, etc.), account for about 5% of the area and hence are regions of high susceptibility for hazard forecasting. Similarly, active eolian dunes and sand ramps located on the east side of Mesquite, Ivanpah, and Hidden Valleys adjacent to playas account for over 3% of the region. Analyses of remotely sensed data and field studies identified previously unmapped fault scarps or queried faults in the Kingston Wash area, Shadow Mountains, southern Pahrump Valley, Bird Spring Range, Lucy Gray Mountains and Piute Valley. Although no definitive Holocene tectonic displacement was observed, ample evidence exists for Pleistocene activity generally oriented with north-northwest strikes.

Acknowledgements

This report is a product of the Surficial Geology Project, funded by National Cooperative Geologic Mapping and Earth Surface Dynamics Programs, U.S. Geological Survey. The authors thank David Miller and Geoffrey Phelps for thoughtful reviews. Conversations with Kyle House of Nevada Bureau of Mines and Geology helped clarify field relations. We gratefully thank our field assistants Leila Gass, Aydin McMackin, and Victoria Langenheim. Stephanie L. Dudash aided with digital preparation of map.

Description of Map Units

Classification of the Quaternary geologic units presented here is based upon previous research by Yount and others (1994), and shares similarities with Birkeland, and others (1991) and Birkeland (1999), such that the first two characters in a unit label designate the relative age followed by a geomorphic process label and a subsequent modifier. The first letter is the period (Quaternary), the second letter is the relative age, the third letter is an abbreviation for the process type, and the fourth letter is reserved for an additional modifier of the process, age, or material. The relative ages of the units are sequentially presented beginning with the youngest surface or deposit. For example, a Qax surface is "active", Qyx is "young", Qix is "intermediate", and Qox is "old"; where x is a placeholder for numerous deposits such as a (alluvium), e (eolian), or p (playa). Unless observed in the field and specifically mapped, it is possible that a given age geologic unit may be composed of a variety of subunits. For instance, alluvial units may have significant contributions from eolian or mass-wasting deposits. Hence subunits such as mass-wasting deposits are more common than represented in the map on plate 1 but could not be reliably deciphered from remote sensing techniques.

Active surfaces have received deposition within the last few decades (Qax) or centuries. They are characterized by loose sediment and are prone to flooding and sediment transport. They are typically unvegetated or moderately vegetated and have rough microtopography such as strongly developed bar and swale or debris-flow morphology such as lobes and levees. Active surfaces are small in area on alluvial fans and form discrete channels. Young surfaces (Qyx) are middle and early Holocene in age but are abandoned or receive sediment infrequently. They are characterized by loose to slightly compact sediments. Soil is thin and weakly developed and typically expressed as an incipient to weak, sandy vesicular horizon (A_v), weak cambic horizons (B_w), and stage I calcic horizons (B_k to B_{km}). Young surfaces are moderately vegetated, especially with shrubs, and have fairly smooth microtopography, with moderate to faint remnants of bar and swale topography. Although no desert pavement or incipient pavement is generally present, the surface clasts have incipient varnish. Intermediate surfaces (Qix) are late and middle Pleistocene in age and have been abandoned for tens to hundreds of thousands of years. Sediments can be loose but are commonly compact. On these intermediate surfaces, desert pavement is moderately to well-developed with moderate to strong varnish on surface clasts of alluvium, except at high altitude. Microtopography of the surface is flat, lacking the original depositional morphology, but may exhibit weak to moderate incision locally. Pedogenic soil is moderately to well-developed with a silty A_v horizon, moderately to strongly developed B_t horizon and calcic stage development of I+ to III+ (Gile and others, 1965, 1966; Machette, 1985). Time-dependent processes such as

pedogenesis, varnish development, and the vertical separation between units were best judged from field relations.

The following unit descriptions are formatted in the following general sequence of 1) grain size, size range, color, and composition, 2) sedimentary structures, rounding, consolidation, 3) surface morphology, 4) soil development, 5) inset relations with other units, 6) characteristic landforms and landscape positions, 7) vegetation characteristics, 8) human implications, and/or any diagnostic features. The following primary categories are grouped by depositional transport process with units presented from in order of increasing age. The corresponding correlation of map units is depicted on plate 1.

Surficial Deposits

Anthropogenic deposits

ml **Made land or artificial fill (latest Holocene)**— Material of varying grain size and composition moved for construction purposes and agricultural disturbance that significantly alters the geologic processes effecting the surface in terms of drainage, stability and soil development. Typically lacks sedimentary structures, surface morphology, and soil development inherited from original deposit. Vegetation is typically sparse

Axial valley deposits

- Qav** **Active valley-axis deposit (latest Holocene)**— Moderately to poorly sorted fine gravel, sand, silt, and clay. Loose and unconsolidated relatively smooth surface that is easily disturbed. Little or no soil development. Fine-grained deposits in valley axes characterized by anastomosing washes, rounded interfluves, and complexly interfingering eolian sediments. Flow direction typically diverges from regional alluvial fan gradients contributing water and sediment to valley axis. Cross-cuts distal alluvial fan transport. Sparsely to moderately vegetated with creosote bush (*Larrea tridentata*), cheesebush (*Hymenoclea salsola*), and black-banded rabbitbrush (*Chrysothamnus paniculatus*). Unit appears light in tone (high albedo) in remote sensing images. Prone to flooding
- Qyv** **Young valley-axis deposit (Holocene and latest Pleistocene)**— Moderately to poorly sorted sand, silt and clay. Loose, somewhat consolidated. Weakly developed soil, expressed as incipient to weak sandy A_v horizon and weak cambic horizon; stage I or no calcic soil typical (calcic stage nomenclature follows Gile and others, 1966 and Machette, 1985). Fine-grained deposits in largely inactive valley axis locations characterized by anastomosing washes, gentle interfluves, and complexly interfingering eolian sediments. Moderately vegetated. Prone to occasional flooding. Located in Shadow Valley and Ivanpah playa
- Qiv** **Intermediate valley-axis deposit (late and middle Pleistocene)**— Medium- to fine-grained sand to silt and clay with interbedded coarse sand to gravel. Generally light tan to light yellow in color. Coarse sand and gravel may provide a darker color

depending on composition. Fine-grained sediments in the inactive valley axis locations characterized by moderate to deeply dissected deposits. Sediments can represent a mix of alluvial, eolian, and groundwater discharge sediments. Appears light gray to white in aerial photographs and light tan to medium brown on the satellite imagery. Located in the Kingston Wash floodplain in Shadow Valley

- Qov Older valley-axis deposits (early Pleistocene)**— Generally interbedded fine to medium grained weakly lithified sandstone interbedded with mudstone and claystone, in beds up to 1 m thick. Pebbly sandstone occurs locally as channel fill deposits. Surface typically mantled with younger units and is exposed in cutbanks in Stump Springs area. Deposit contains buried soils and bedding is inclined at dips up to 35°. Fine-grained sediments in the axial part of Pahrump Valley exposed beneath intermediate age alluvial and groundwater discharge deposits. Quade and others (1995) noted that much of the older Quaternary deposits resulted from groundwater discharge, though the unit also contains significant portions of eolian and alluvial deposits representing other depositional processes. Mapped as older valley-axis deposits in recognition of the mixed modes of deposition represented in this unit. Lundstrom and others (2003) obtained thermoluminescence dates on similar basin fill material (lower part of basin-fill of Browns Spring in Mound Spring Quadrangle) of 275–400 ka

Wash deposits

- Qaw Active wash deposit (latest Holocene)**— Moderately to poorly sorted sand and gravel. Loose and unconsolidated, easily disturbed. Little or no soil development. Up to several meters of active sediments deposited within the last few decades. Generally lacks vegetation on surfaces active with water flow and sediment transport on semi-annual basis or moderately vegetated on surfaces or channels active on decadal basis with creosote bush (*Larrea tridentata*), cheesebush (*Hymenoclea salsola*), black-banded rabbitbrush (*Chrysothamnus paniculatus*), as well as catclaw (*Acacia greggii* var. *arizonica*) and honey mesquite (*Prosopis glandulosa*) at higher elevations

- Qawg Active wash deposit dominantly composed of grus (latest Holocene)**— Moderately well sorted sediment ranging in size from coarse sand to fine gravel. Composed predominately of clasts from granitic source that weathers to grus. Sedimentary structures are typically lacking and surface morphology is subdued. Unit appears light in tone (high albedo) in remote sensing images. Prone to flooding. Mapped mainly where ephemeral stream is present as continuous non-anastomosing thread

Alluvial and debris-flow deposits

- Qaa Active alluvial fan deposit (latest Holocene)**— Poorly sorted mixed clastic sediment ranging from fine sand to boulders. Typically uncemented and unconsolidated, easily disturbed. Surface undulating with diffused microtopography common to braided streams or pronounced bar and swale topography; little channel incision

exists. Little or no soil development but may have a significant eolian component, especially in distal fan zones adjacent to deposits of fine-grained sediment. Alluvial fan deposits characterized by surfaces and channels actively receiving sediments within the last few years or decades by ephemeral streams. May be prone to flooding. Vegetation typically reflects the age of surfaces with primarily annuals on recently active deposits whereas surfaces active on decadal basis are moderately vegetated with shrubs such as creosote bush (*Larrea tridentata*) (fig. 16)

Qaag

Active alluvial fan deposit composed of grus (latest Holocene)— Alluvial fan material composed predominately of clasts from granitic sources that weather to grus. Moderately well sorted sediment ranging in size from coarse sand to fine gravel. Sedimentary structures are typically lacking and surface morphology is subdued. Inset surface relations are commonly less than 0.5 m from active wash to highest surface. Little fining of clast size with distance from mountain front

Qya

Young alluvial fan deposit (Holocene and latest Pleistocene)— Poorly to moderately sorted mixed clastic sediment ranging from fine sand to boulders. Poorly cemented and consolidated. Loose to slightly compact. Alluvial fan deposits characterized by surfaces that are abandoned or receive materials infrequently with sporadic channel avulsions in downstream-branching ephemeral streams. Fairly rough microtopography in much of fan, with moderate to faint remnants of bar and swale topography. No desert pavement or weak pavement (fig. 15). Incipient to weak varnish on clasts. Weakly developed soil, expressed as incipient to weak sandy A_v horizon and weak cambic horizon; stage I or no calcic soil typical (calcic stages follow Gile and others, 1966 and Machette, 1985). Moderately to sparsely vegetated, especially with creosote bush (*Larrea tridentata*), Cheesebush (*Hymenoclea salsola*) in more active units, Mormon tea (*ephedra spp.*) at higher altitudes and other smaller shrubs such as white bursage. Although rodent burrows are ubiquitous throughout the map region, they tend to be denser within Qya deposits, especially surrounding creosote bushes. May have locally dense soil crust assemblages (fig. 27)

Qyao

Older young alluvial fan (early Holocene and latest Pleistocene)— Alluvial fan deposits characterized by small patches of weakly to moderately developed pavement with weak varnish on clasts that develop varnish. Soil development consists of 1 to 4 cm thick A_v horizon, weak cambic to B_{tw} horizon, stage I to II calcic development. Deposits typically inset into intermediate aged deposits and are incised by active deposits. As this unit cannot be reliably determined solely from remote sensing techniques, it is mapped only where determined from field study (located near Jean Lake and Stateline Pass); deposits are much more widespread than shown

Qyag

Young alluvial fan deposit composed of grus (Holocene and latest Pleistocene)— Alluvial fan composed of clasts ranging in size from coarse sand to fine gravel from a granitic source that weathers to grus. Surface undulating and smooth; little channel dissection. Pavements, varnish, and soil development immature. If present, incipient A_v horizon is sandy, cambic horizon is poorly developed, and calcic horizon development of stage I to II. Soil development is commonly weaker and tends to be less incised near mountain fronts than unit Qya.

Especially common downslope of gneissic Early Proterozoic granitoids and associated pegmatitic dike outcrops

- Qyaog** **Older young alluvial fan composed of grus (early Holocene and latest Pleistocene)**— Older young alluvial deposits made up of clasts from granitic sources that weather to grus, characterized by weakly developed pavements that generally lack varnish. Soil development is weaker than Qyao, particularly as weak sandy A_v horizons. Mapped only where determined from field study (principally located in Ivanpah Valley between Clark Mountain and the Lucy Gray Mountains); deposits are much more widespread than shown
- Qyad** **Young alluvial fan composed of debris-flow deposits (Holocene and latest Pleistocene)**— Young alluvial deposits dominated by debris flows characterized by randomly distributed boulder-rich clasts distributed in a fine-grained matrix. Lenses of moderately sorted and weakly bedded fine-grained material may occur within large deposits where material is more fluid. Deposit surfaces express high roughness with pronounced steep-sided levees, depositional lobes with a concentration of coarse particles near the surge front, and boulder-studded interiors. Locally deposits may overtop banks leaving a concentration of coarse clasts or trigger a channel avulsion. Likely includes a range of transport processes including hyperconcentrated flows. Mapped only where determined from field observations; deposits are much more widespread than shown
- Qia** **Intermediate alluvial fan deposit (late and middle Pleistocene)**— Poorly- to moderately-sorted silt, sand, gravel, cobbles, and boulders. Light to dark brown surface with mostly subangular to sub-rounded clasts (fig. 12) that coarsen in size toward mountain fronts. Typically compact but can be loose from bioturbation. Alluvial fan deposits characterized by surfaces devoid of relic bar and swale topography that have been abandoned for tens of thousands of years. Moderately to well developed interlocking desert pavement with moderate to strong varnish on clasts, and flat smooth surface that is partly incised by narrow channels. Well-developed platy A_v horizon (>5 cm thick) composed of silt, very fine sand, and clay (fig. 14). Moderately to strongly developed argillic B_t horizon and stage I+ to III+ calcic horizon. B_{tk} may be present in older, more deeply incised deposit with diffused edges. Pavement, varnish, and A_v horizon subdued to absent at high altitudes (above approximately 1100 m); B_t horizon thicker at high altitude, calcic horizon thin. Correlated to unit Qia3 of Yount and others (1994) based on evidence for surface degradation and soil development. Very sparsely vegetated, locally with widely spaced creosote bush, Mojave yucca (*Yucca shidigera*), or Buckhorn cholla (*Opuntia acanthocarpa* var. *coloradensis*). Vegetation density positively correlated with altitude. Bioturbation associated with high elevation sites where black brush (*Coleogyne ramosissima*) is abundant tends to inhibit pedogenesis and in some areas Qia may be distinguished on other criteria such as geomorphic position and weathering of surface clasts
- Qia** **Intermediate alluvial fan deposit composed of grus (late and middle Pleistocene)**— Alluvial fan made up of clasts from granitic source that weathers to grus. Surface morphology is broadly undulating with rounded surfaces. Compared to general unit Qia, Qia generally lacks or has a very poorly developed pavement and poor desert varnish. The A_v horizon is sandy, the B_t horizon is moderately to

well developed, and the calcic horizon development is limited to stage I to II. Although diagnostic inset relations are rare, exposed argillic horizons within inset younger channels denote the surface is being incised

- Qiad Intermediate alluvial fan composed of debris-flow deposits (late and middle Pleistocene)**— Intermediate alluvial deposits dominated by debris flows; poorly sorted bouldery deposits with sand and silt matrix. Sedimentologic characteristics similar to Qyad except that pavement and pedogenic character similar to Qia deposits. Boulder size tends to exceed that found in Qyad deposits. Mapped only where verified by field observations and hence deposits are more widespread than shown
- Qoa Old alluvial fan deposit (middle and early Pleistocene)**— Silt, sand, gravel, and cobbles. Light colored surface with mostly subangular to sub-rounded clasts that coarsen in size toward mountain fronts. Compact to cemented. Commonly forms pale-colored ballenas above active washes in upper parts of alluvial fans near mountain fronts. Many clasts on surface commonly made up of disaggregated pieces or platelets of petrocalcic soil horizon. Most upper soil horizons stripped off by erosion but commonly has superimposed weak soils developed directly on calcic horizon (fig. 11). Locally may have remnant varnished pavement clasts at the surface, including disaggregated pieces of calcic horizon, with a very thin or absent B_t horizon suggesting the surface once had pavement characteristics that have since degraded. Stage IV and greater calcic horizons 2 to 6 m thick. Forms rounded, deeply dissected terrane with little or no remnant depositional geomorphology; a few meters to tens of meters higher than surrounding surfaces. Characterized by degraded remnants of abandoned surfaces forming boulder-studded ridges. Moderately vegetated. Qoa deposits dominate south of Las Vegas in the northern McCullough Mountains and form high, somewhat flat to rounded ridges with scattered B_t horizons on thick stage IV + calcic horizons. In the Kingston Range, two sub units of Qoa occur. The younger unit has a single stage IV calcic horizon with boulders up to several meters thick. The older unit includes several calcic horizons approaching stage V development. Good example of these sub units is in the Qoa fans at the mouth of the canyon draining northward from Tecopa Pass and along the north fork of Kingston Wash
- Qoag Old alluvial fan deposit composed of grus (middle and early Pleistocene)**— Old alluvial fan made up of clasts from granitic source that weathers to grus; surface commonly is active and does not show A_v horizon; topography incised; B_t horizon rarely remains, calcic horizon pronounced. Sedimentologic characteristics similar to Qiad except deposit tends to be more deeply incised. Numerous deposits in valley between Lucy Gray Mountains and McCullough Range
- Qoad Old alluvial fan composed of debris-flow deposits (middle and early Pleistocene)**— Old alluvial deposits dominated by debris flows; poorly sorted bouldery deposits with sand and silt matrix. Sedimentologic characteristics similar to Qyad except that pavement and pedogenic character similar to Qoa deposits. Boulder size tends to exceed that found in Qyad deposits. Mapped only where verified by field observations and hence deposits are more widespread than shown
- QToa Oldest Quaternary-Tertiary alluvial fan deposit (early Pleistocene and Pliocene)**— Silt, sand, gravel, and cobbles, and boulders. Compact to cemented. Mixed clast

composition. Lacks remnants of abandoned surfaces or soil horizons. Moderately vegetated. Forms deeply dissected, typically steep, terrane with little or no remnant depositional geomorphology; deposits generally did not form in present topography, as indicated by source directions or clast composition. Largely undivided with respect to depositional process. May have several sets of paleosols exposed in wash-cut profiles. Younger, superimposed, soil horizons locally present. Lacks consolidation and cementation of unit pc. Most deposits located in Shadow Mountains, south fringe of Kingston Range, and Piute Valley. Age constraints uncertain

Eolian deposits

- Qae** **Active eolian sand deposit (latest Holocene)**— Pale brown to light gray, moderately- to well sorted, moderately bedded, sand with sparse clasts. Loose and subject to migration. No soil development. High albedo on aerial photography. Generally lacks vegetation but some undifferentiated units include sand sheets and low (<0.5 m) shrub mounds. Contacts with neighboring units are gradational
- Qaed** **Active eolian sand dune deposit (latest Holocene)**— Pale brown to light gray, moderately- to well sorted, moderately bedded, sand with sparse clasts. Loose and subject to migration but preserves dune morphology of lee and stross slopes separated by sharp crest. No soil development. High albedo on aerial photography. Generally lacks vegetation but may have shrub mounds. Contacts with neighboring units are gradational. Dune deposits of free-formed sand on the southeast edge of Mesquite Lake where active dunes formed at the southeast-edge of the dunes in southeast Mesquite Valley
- Qaer** **Active eolian sand ramp deposit (latest Holocene)**— Ramp (climbing and falling dunes) deposits generally deposited over inclined bedrock surface (fig. 19). Most active eolian sand deposits occur near local sand sources such as playas or playa fringes. Contacts with neighboring units are gradational
- Qye** **Young eolian sand deposit (Holocene and latest Pleistocene)**— Pale brown, moderately to well-sorted sand deposits with sparse clasts that are generally inactive. Appears as slightly darker albedo surface than high albedo Qae unit. Loose. Sparsely vegetated
- Qyed** **Young eolian sand dune deposit (Holocene and latest Pleistocene)**— Dune deposits; locally comprises mesquite coppice dunes, up to 30 m high, on the east side of Mesquite Valley bolson and near Stump Spring along the fault scarp of the Stateline fault. Dunes are commonly stabilized by mature honey mesquite (*Prosopis glandulosa*) trees. In the southern Mesquite Valley dunes are composed largely of gypsum and have a gypsum-cemented surface crust up to 0.5 cm thick. This crust appears to have stabilized the deposits and limited the remobilization of sand. In the Stump Spring area, without the influence of the gypsum cement, there are moderate amounts of active sand, not distinguished in this map
- Qie** **Intermediate eolian sand deposit (late and middle Pleistocene)**— Pale brown to reddish well-sorted sands that are inactive. Moderately compact and weakly cemented. Bedding is typically parallel and massive with abundant root casts suggesting sand accumulation on vegetated plain with episodic groundwater

discharge to drive the formation hydromorphic soils. Low relief surface commonly covered with deflation pavement of coarse sand, pebbles and carbonate chips. Characterized by one or more B_t horizons and calcic (B_{km}) horizons. Locally intensive bioturbation occurs in rodent mounds that are commonly excavated by predators. In most areas the Qie pavement surface is overlain by Holocene to active vegetation mounds and small dunes up to 1 m. On the north side of Kingston Wash, Qie deposits are covered by low Qye dunes stabilized by vegetation, principally grass. The vegetation-stabilized dunes lie over a sandy unit commonly armored with gravel and nodules of soil carbonate. In vertical exposures, particularly in the deep tributary on the north side Kingston Wash, near Coyote Holes spring, Qie deposits cap an older sequence of similar sands to form the top layer of aggrading eolian sand. The top sand unit is 2 to 3 m thick in massive to thick bedded layers with soil development to 1.5 m depth. Calcium carbonate development is stage III and ~0.5 m thick, composed of isolated to coalesced nodules with minor laminations on the top and isolated nodules below the base of the main layer, occurs approximately 1 m below the surface

- Qoe Old eolian sand deposit (middle and early Pleistocene)**— Pale brown to reddish, well-sorted sand filling paleo-valley on the piedmont north of Kingston Wash. Sand is moderately to poorly cemented and easily eroded. Well-exposed in the vertical walls of a deep canyon north of Coyotes Holes spring where section is approximately 30 m thick, composed of a succession sandy soils with well-cemented stage IV carbonate layers up to 1 m thick with intergrown nodules and laminae. Differential weathering and extensive insect burrowing is common. The older sand unit contains multiple paleosols marked by remnant B horizons with reddish-brown sand over massive carbonate-cemented sand layers up to 2 m thick. Where this unit is exposed, in uplifted fault blocks north of Kingston Wash, the sand is deeply eroded exposing massive carbonate-cemented sand with abundant nodular carbonate on the surface. Age constraint is poor. Observed solely in Kingston Wash

Mixed alluvial and eolian deposits

- Qaa Active mixed alluvial and eolian sand deposit (latest Holocene)**— Lithologically and morphologically similar to unit Qaa with secondary eolian deposits. Gravelly sand with vague to well-defined thin bedding. Loose. Alluvial and eolian sediments that are thoroughly mixed, with alluvial processes dominant. Active deposition of eolian sand is secondary but present throughout deposit. Forms flatter surfaces than alluvial systems lacking significant eolian sand because eolian sand additions mute topography. No soil development. High albedo on aerial photography. Vegetation mounds and small dunes common. Contacts with neighboring units are gradational
- Qyae Young mixed alluvial and eolian sand deposit (Holocene and latest Pleistocene)**— Lithologically and morphologically similar to unit Qya with secondary eolian deposits. Alluvial and eolian sediments that are thoroughly mixed, with alluvial processes dominant. Gravelly sand with vague to well-defined thin bedding. Loose. Forms flatter surfaces than alluvial systems lacking significant eolian sand because eolian sand addition mutes topography. Little or no soil development. Appears as

slightly darker surface than high albedo Qae surfaces. Sparsely vegetated, generally supporting creosote bush. Contacts with neighboring units, typically Qyea or Qya, are gradational

- Qyea** **Young mixed eolian sand and alluvial deposit (Holocene and latest Pleistocene)**— Lithologically and morphologically similar to unit Qye with secondary alluvial deposits. Eolian and alluvial sediments that are thoroughly mixed, with eolian processes dominating. Gravelly sand with vague to well-defined thin bedding. Loose. Alluvial channels muted or invisible; deposit mostly sand with sparse gravel. Forms broad, flat surfaces. Little or no soil development. Sparsely vegetated, generally with no creosote bush, grasses common. Generally in distal fan environment. Prone to surface modification by eolian sediment transport. Located southeast of Ivanpah Lake. Contacts with neighboring units are gradational
- Qiae** **Intermediate mixed alluvial and eolian sand deposit (late and middle Pleistocene)**— Lithologically and morphologically similar to unit Qia, although eolian sand is thoroughly mixed throughout deposit, with alluvial processes dominating. Gravelly sand with vague to well-defined thin bedding. Moderately compact. Forms flat surfaces in the distal fan zone adjacent to valley axis deposits that are the main source of eolian sediment. Somewhat retarded pedogenic characteristics such as inconsistently developed pavement and varnish, B_t horizon, and calcic horizon. Pavement surfaces may be composed of ventifacts. Moderate to sparse vegetation. Exposures east of Jean Lake contain abundant accumulations of red sand derived from Permian red sandstones
- Qoae** **Old mixed alluvial and eolian sand deposit (middle and early Pleistocene)**— Lithologically and morphologically similar to unit Qoa, although eolian sand is thoroughly mixed throughout deposit, with alluvial processes dominating. Gravelly sand with vague to well-defined thin bedding. Moderately compact. Forms flat surfaces. Location not necessarily correlated with modern source of eolian sediment. Somewhat retarded pedogenic characteristics such as inconsistently developed pavement and varnish, B_t horizon, and calcic horizon. Pavement surfaces may be composed of ventifacts. Moderate to sparse vegetation. Located in Kingston Wash

Playa deposits

- Qap** **Active playa deposit (latest Holocene)**— Weakly bedded, poorly sorted silt, clay, and sand; locally salt rich. Predominately dry playas actively receiving water and sediment from surrounding source areas within the last few decades. Thin to thick sub-horizontal bedding. Mud-cracked; in places cut by linear fissures that support vegetation. Compact. Generally flat, sparse or no vegetation. Light in color on aerial photography. Prone to flooding (fig. 22); receives stream flow and standing water, and is subject to eolian deposition and erosion (Figures 18-21). Langer (1965) reported that i) dry crusts are hard, compact, and physically coherent, ii) precipitation does not ordinarily penetrate more than several mm, iii) silt fractions under 5 microns increases porosity and bearing strength, and iv) playas with > 50% clay-size particles possess extensive desiccation cracks

- Qaps** **Active playa sandy facies deposit (latest Holocene)**— Sandy facies of playa that typically supports sparse vegetation, generally near margin of playa where alluvial sediments interfinger with playa sediments
- Qapf** **Active playa fringe deposit (latest Holocene)**— Pale brown to light gray, poorly- to well-sorted silt, clay, and sand. Loose and unconsolidated. Complexly mixed material of eolian, lacustrine, playa, alluvial, and groundwater discharge origins form halo around playas modified by prevailing wind directions. Diffused, undulating surface morphology muted by eolian silt and sand input sourced from local playa. No soil development. High albedo on aerial photography. Vegetation dominated by grasses with few shrubs. Prone to frequent surface modification by eolian sediment transport. Particularly extensive on margins of Roach and Jean Lakes
- Qypf** **Young playa fringe deposit (Holocene and latest Pleistocene)**— Pale brown to light gray, poorly- to well-sorted silt, clay, and sand. Loose and unconsolidated. Complexly mixed material of eolian, lacustrine, playa, alluvial, and groundwater discharge origins form halo around playas, modified by prevailing wind directions. Diffused, undulating low gradient surface moderately well-vegetated by grasses with sparse creosote bush. Little to no soil development. Infrequently active as indicated by minor channeling of dry surface. Vegetation dominated by grasses with few shrubs. High albedo on aerial photography. Prone to surface modification by eolian sediment transport
- Qapw** **Active wet playa deposit (latest Holocene)**— Morphologically similar to unit Qap but added groundwater discharge generates lithologic diversity. Designation derived from Rosen (1994). Extensive gypsiferous silts and muds occurring in the soil and subsoil sediments on the valley floor. Gypsum crystals weather from the outcrop. Local efflorescence of salts. Various species of saltbushes (*Atriplex*) dominant. Moderate to high soil moisture. Sites distinguished as zones of active groundwater discharge at the time of field work in November 2003. Observed in Mesquite Valley where active playa deposits at Mesquite Lake have low clay content but abundant gypsum (figs. 24 and 25). Russian Thistle (*Salsola iberica*) present in disturbed areas. Although active deposition appears to require shallow groundwater, the involvement of encrusting evaporite salts distinguish this unit from groundwater discharge deposits as described by Quade and others (1995). Late Paleozoic rocks exposed in the Stateline Pass area and on the west slope of the Spring Mountains are the mostly likely source of the gypsum in this basin. The gypsum is probably transported from bedrock areas in groundwater as calcium sulfate, although once precipitated in the shallow surface deposits, it can be remobilized by eolian transport. Prone to flooding and eolian dust storms
- Qypw** **Young wet playa deposit (Holocene and latest Pleistocene)**— Lithologically and morphologically similar to unit Qapw but less frequent addition of water and sediment. Refers chiefly to ground-water discharge type playa deposits in northern Mesquite Valley. Generally fine-grained sand and silt to sandy clay loam, light tan to light yellowish brown. Massive sand with a weakly cemented surface crust over several centimeters of loose sand and silt over a moderately compact, sand and slit with gypsum cement. The crusted surface is irregular, with evidence of disturbance and recementation of the crust. Commonly incised by local drainage with

vegetation mounds of eolian sand up 1 m in height. Distinguished from Qapw by the lack of surface moisture at the time of observation and absence of significant recovery of the surfaces in disturbed areas

- Qipw Intermediate wet playa deposit (late and middle Pleistocene)**— Lithologically and morphologically similar to unit Qypw but with pronounced pedogenesis. Light brown to pinkish gray A horizon up to 0.5 m thick over B_y horizon up to 0.5 m thick with gypsum cement making B_y horizon slightly more resistant and difficult to dig. Petrogypsic horizon is likely progressively developed with age so that Qia paleosols may be as much as 1 m thick. Section is dominated by clastic sediment in the medium-grained sand to silt and clay range. Gypsum may coexist with an efflorescence of white salt on the exposed B_y horizon. Sediment below the B horizon exhibits similar grain size in the range from medium sand to silt and clay. Possible depositional settings include vegetation trapping eolian sediment and valley axis fluvial transport. Salt weathering *in situ* may contribute to grain size reduction and increasing clay content but the absence of coarser fractions indicates that the sediment was relatively fine grained upon deposition. Locally buried soils were observed
- Qipc Intermediate crystal body playa deposit (late and middle Pleistocene)**— Weakly bedded, poorly sorted silt, clay, and sand; locally dominated by salts. Compact. Tan to yellowish tan mud with crystalline gypsum, up to an estimated 60% by volume, in beds up to 1 m thick. Intergrown crystals with inclusions of mud indicate displaced crystal growth, as described by Motts (1965), where crystallization occurs in salt saturated groundwater below the surface of the playa. In southern Mesquite Valley eolian deflation of 1 to 2 meters of late Pleistocene wet playa deposits has revealed an underlying, previously buried, crystal body playa. The surface of the crystal body playa deposits is commonly covered with abundant crystals of selenite gypsum up to 5 cm in length. The structure of the subsurface layers is revealed in several prospect-development trenches in the middle part of the playa (figs. 24 and 25)
- Qil Intermediate lacustrine deposit (late and middle Pleistocene)**— Pluvial lake sediments. Buried lacustrine sediment along southwestern edge of Ivanpah Lake is reddish muddy sand that may represent the most recent pluvial cycle, but is undated

Groundwater discharge deposits

- Qags Active groundwater discharge deposit (latest Holocene)**— Predominately sand and silt, moderate brown to reddish brown, typically formed of a mixture of gravelly sand from distal alluvial fans and eolian sand and silt from adjacent valley deposits. Unit includes distal fan deposits that exhibit evidence of groundwater discharge where the water table approaches and intersects the ground surface. The vegetation supported by the available groundwater acts as significant component in the system by trapping and retaining sediment. Located in the area around Kingston Spring
- Qygs Young groundwater discharge deposit (Holocene and latest Pleistocene)**— Silt and fine sand in zones of former groundwater discharge. Commonly forms light-colored, flat areas or dissected badlands. Loose to compact. Observed in the distal fan transition zone on the fan complex draining east from Kingston Peak where the

vegetation appears to be declining in health and near bedrock exposures in the northern tip of the Lucy Gray Mountains. Mound deposits at Potosi Spring have been disturbed by attempts at anthropogenic water development

- Qig Intermediate groundwater discharge deposit (late and middle Pleistocene)**— Silt and fine sand in former zones of groundwater discharge; source processes unidentified. Generally white to light brown; compact. Contains one or more pedogenic calcic horizon, stage III to IV. Little vegetation, generally dissected. Quade and others (1995) identified 4 facies of alluvial fan/groundwater discharge units in the Pleistocene record at Corn Creek, Nevada; including (1) upper alluvial fan with coarse-grained porous sediment, deep water table, and xerophytes, (2) phreatophyte flat with sand to silt, shallow groundwater, and phreatophyte plant species, (3) wet meadow with gley muds, springs, and equivalent meadow plant species, (4) marsh with mud, open standing water, and wetland plant species. Groundwater deposits identified on this map include part of the phreatophyte and wet meadow facies. None of the sections identified in this mapping has specific evidence of the marsh facies with open water. However active zones of groundwater discharge are indicated by phreatophyte and wet meadow vegetation in distal fan zones, but evidence is not preserved in Pleistocene deposits. Intermediate aged groundwater discharge deposits mapped in this quadrangle include Stump Spring area, upper Sandy Valley, and upper Kingston Wash. Quade and others (1995) included Qig deposits in southern Pahrump Valley and northeastern Mesquite Valley as typical examples of groundwater discharge deposits at Stump Spring and upper Sandy Valley as typical examples of distal fan discharge deposits. Groundwater discharge deposits at both sites are fault controlled
- Qog Old groundwater discharge deposit (middle and early Pleistocene)**— Calcareous silt and fine sand in former zones of groundwater discharge; source processes unidentified. Generally white, light brown, to slightly reddish; compact although lower bulk density than pedogenic carbonate horizon. Contains ostracode fossils. High albedo surface on remote sensing images. Located in Bird Spring Range along lineaments and in Stump Spring along fault zone

Erosional surfaces and deposits on erosional surfaces

Hillslope environment

Hillslopes are characterized by patchy distributions of bare rock, thin deposits weathered from rock, and materials transported short distances by gravity and carried by water. Hillslope deposits are labeled uniformly regardless of the transport mechanism. The spatial distribution is typically irregular although thicker, aerially consistent units were distinguished as colluvium. Divided into:

- Qymc Young colluvial deposits (Holocene and latest Pleistocene)**— Colluvial materials thicker than 2 m covering a wide area; exact age undetermined. Rocky and poorly sorted, mixed detritus ranging from boulders to silt and clay. Massive to very poorly bedded, angular clasts. Loose to moderately compact with composition directly reflecting source areas upslope. Weak to moderate soil development

- depending on the availability of fine-grained sediment. Landforms range from angular talus slopes to concave up slopes that grade into low angle alluvial fans
- Qimc Intermediate colluvial deposits (late and middle Pleistocene)**— Colluvial materials thicker than 2 m covering a wide area. Rocky and poorly sorted, mixed detritus ranging from boulders to silt and clay. Massive to very poorly bedded, angular clasts. Deposit surfaces are generally smooth with sharply incised gullies. Moderately compact to compact with surface generally dark with desert varnish or moderate to deep etching depending on clast lithology. Soils may have up to 5 cm thick A_v horizons and moderate to strong reddening of the upper B horizon. Strongly developed B_t horizon and local development of stage II to III pedogenic calcic horizon, typically less developed than calcic horizons in alluvial deposits of similar age. Soil development appears to depend on availability of fine-grained sediment to fill in among the coarse clasts. Composition reflects upslope source area. In some areas deposits form relatively uniform steep slopes covered with a surface of darkly varnished boulders. Excellent exposures south of Kingston Range in Shadow Mountains and east of McCullough and Highland Ranges
- Qomc Older colluvial deposits (middle and early Pleistocene)**— Poorly sorted, mixed detritus ranging from boulders to silt and clay. Composition reflect source areas upslope. Massive to very poorly bedded, angular clasts. Surfaces are typically deeply incised with rounded crests between gullies. Compact with soils generally stripped to the carbonate cemented portion of the B horizon. Clasts are deeply weathered and many have carbonate coatings that indicate the rocks have moved from their original position in the soil. Generally lighter in color (higher albedo) than intermediate aged colluvial deposits (Qimc). Primarily located in northeast Kingston Range
- Qha Abundant hillslope deposits (Holocene and Pleistocene)**— Hillslope materials such as colluvium, talus, regolith, and landslide deposits; aerial extent of cover greater than rock. Generally less than 2 m thick or patchy distribution with small fraction of area covered by deposits thicker than 2 m. Unit does not occur in isolation but in conjunction with bedrock substrate type
- Qhs Sparse hillslope deposits (Holocene and Pleistocene)**— Hillslope materials such as colluvium, talus, regolith, and landslide deposits; aerial extent of cover less than rock. Generally less than 2 m thick with patchy distribution. Unit does not occur in isolation but in conjunction with bedrock substrate type

Pediment surfaces

Gently-sloping erosional surfaces in various stages of erosion and burial. Generally forms in felsic granite that weathers to grus (**fpg**) and partly consolidated (**pc**) materials. Substrate materials indicated after hyphen (-) in unit symbol. Good examples of pediments can be found in the Kingston Range and northern Lucy Gray Mountains. Divided into two general classes defined by the degree of dissection:

- Qpi Incised pediment**—Incised pediment with most of the surface expressed as flat exposures of bare rock with patchy cover of veneer; channels cut into rock transport eroded sediment. Located in northern portions of the Kingston Range, Mesquite

Mountains, and Lucy Gray Mountains

Qpd Deeply dissected pediment—Deeply dissected pediment identifiable by similar heights of isolated parts expressed in bedrock pinnacles. Area between pinnacles may be covered with sediment or nearly bare rock. Located solely on east flank of Mesquite Mountains

Bedrock substrate materials (Tertiary and older)

Shallowly buried rock and partly consolidated materials that lie under surficial deposits, and under pediment and hillslope veneers. Ages range from Pliocene to early Proterozoic. Bedford and Miller (1998) is the primary source of digital bedrock mapping data. Bedrock in the western half of the quadrangle is taken largely from unpublished mapping of bedrock by McMackin. The following rock types are subdivided into categories based on initial chemical composition, weathering characteristics, and erosional products.

- ca Carbonate rocks**—Carbonate-mineral rocks such as marble, dolomite, and limestone. Weathered materials commonly include silt
- fp Felsic plutonic rocks**—Plutonic rocks greater than about 68% SiO₂, such as granite and granodiorite
- fpg Felsic plutonic rocks that weather to grus**—Plutonic rocks greater than about 68% SiO₂, typically Tertiary in age, such as granite and granodiorite that weather to angular, coarse-grained fragments resulting from granular disintegration. Also includes Precambrian gneissic and granitic rocks in the McCullough Range (Longwell and others, 1965) that weather to produce material resembling grus
- fv Felsic volcanic rocks**—Volcanic rocks greater than about 68% SiO₂, such as rhyolite, rhyodacite, and felsite. Includes flows and ejecta. Weathered materials include quartz, feldspar, and clay
- mp Mafic plutonic rocks**—Plutonic rocks less than about 68% SiO₂, such as gabbro, diorite, monzodiorite, syenite, and alkalic rocks. Weathered materials chiefly feldspar, amphiboles, and micas
- mr Metamorphic rocks**—Metamorphic rocks of complexly mixed lithology, such as gneiss, migmatite, and structurally mixed rocks. Weathered materials variable
- mv Mafic volcanic rocks**—Volcanic rocks less than about 68% SiO₂, such as dacite, andesite, and basalt. Includes flows and ejecta. Weathered materials include common clay; alluvial fans with mafic volcanic source typically boulder rich
- pc Partly consolidated**—Moderately to weakly consolidated sedimentary deposits; locally includes volcanic rocks or highly altered rocks. Typically Tertiary in age. May form badland topography. Weathered materials include common silt and clay. May be mapped as QToa where depositional process was inferred or age constraints are poor
- sl Siliciclastic rocks**—Silicic sedimentary and metamorphic rocks, such as sandstone and quartzite, shale, and siltstone. Weathered materials commonly include quartz, silt, and clay

Composite symbols

Surficial geologic units commonly exist as thin (<2 m) veneers over older units including bedrock. In areas where this relationship is common, the unit designators are shown on the map separated by a slash (/). The younger, or overlying, unit is indicated first. Thus, Qya/Qoa indicates an area where a veneer of young alluvial fan deposits overlies old alluvial fan deposits and Qya/fpg indicates an area where a veneer of young alluvial fan deposits overlies felsic plutonic rock that weathered to grus. An example of Quaternary deposits (Qoa) over bedrock (ca+sl) (Qoa/ca+sl) is depicted in figure 4.

The lateral extent of individual deposits is commonly so small that each deposit cannot be shown individually at the database map scale. Areas made up of deposits too small to show individually, are indicated by deposits (representing more than 20% of the area) separated by a plus sign (+), with the most common deposit listed first. Thus, Qya + Qia indicates an area with both Qya and Qia deposits and associated surfaces, and that Qya is more common than Qia; other deposits in the area compose less than 20%. Where a slash separates mixed units, the assemblage of mixed units combined by (+) sign are treated as a unit. For instance the unit Qaae/Qaa+Qya indicates that Qaae overlies the mixed unit Qaa+Qya. Similarly, Qia+Qya/Qoa indicates that the mixed unit Qia+Qya overlies Qoa.

References Cited

- Albritton, C.C., Jr., Richards, A., Brokaw, A.L., and Reinemund, J.A., 1954, Geologic controls of lead and zinc deposits in Goodsprings (Yellow Pine) District, Nevada: U. S. Geological Survey Bulletin B 1010, 111 p.
- Anderson, R.E., Crone, A.J., Machette, M.N., Bradley, L.A., and Diehl, S.F., 1995, Characterization of Quaternary and suspected Quaternary faults, Amargosa area, Nevada and California: U.S. Geological Survey Open-File Report 95-0613, 44 p.
- Armstrong, R.L., 1968, Sevier orogenic belt in Nevada and Utah: Geological Society of America Bulletin, v. 79, no. 4, p. 429-458.
- Bedford, D.R., and Miller, D.M., 1998, Bedrock geology database for the Mojave Desert ecoregion: U.S. Geological Survey unpublished digital compilation, 16 p.
- Belnap, J., Rosentreter, R., Leonard, S., Kaltenecker, J.H., Williams, J., and Eldridge, D., 2001, Biological soil crusts: ecology and management: Bureau of Land Management BLM Technical Reference 1730-2001, 119 p.
- Bingler, E.C., and Bonham, H.F., 1972, Reconnaissance geologic map of the McCullough Range and adjacent areas, Clark County, Nevada, Nevada Bureau of Mines Map 45, 1:125,000 scale.
- Birkeland, P.W., 1999, Soils and Geomorphology (3rd ed.): New York, New York, Oxford University Press, 430 p.
- Birkeland, P.W., Machette, M.N., and Haller, K.M., 1991, Soils as a tool for applied Quaternary geology: Utah Geological and Mineral Survey Miscellaneous Publication 91-3, 63 p.
- Bowyer, B., Pampeyan, E.H., and Longwell, C.R., 1958, Geologic map of Clark County, Nevada, U.S. Geological Survey Mineral Investigations Field Studies Map MF-0138, 1:200,000 scale.
- Briere, P.R., 2000, Playa, playa lake, sabkha: Proposed definitions for old terms: Journal of Arid Environments, v. 45, p. 1-7.

- Bull, W.B., 1991, Geomorphic response to climate change: New York, Oxford University Press, 326 p.
- Burchfiel, B.C., and Davis, G.A., 1971, Clark Mountain thrust complex in the Cordillera of southeastern California: geologic summary and field trip guide, *in* Geologic summary and fieldtrip guide, Guidebook field trip 1: Riverside, California, Geological Society of America, Cordilleran Section, p. 1-28.
- Burchfiel, B.C., Fleck, R.J., Secor, D.T., Vincelette, R.R., and Davis, G.A., 1974, Geology of the Spring Mountains, Nevada: Geological Society of America Bulletin, v. 85, p. 1013-1022.
- Calzia, J.P., Frisken, J.G., Jachens, R.C., McMahon, A.B., and Rumsey, C.M., 1987, Mineral resources of the Kingston Range wilderness study area, San Bernardino County, California: U. S. Geological Survey Bulletin 1709-D, 21 p.
- Calzia, J.P., Troxel, B.W., Wright, L.A., Burchfiel, B.C., Davis, G.A., and McMackin, M.R., 2000, Geologic map of the Kingston Range, southern Death Valley, California, U.S. Geological Survey Open-File Report 00-0412, 1:31,680 scale.
- Carr, M.D., 1980, Upper Jurassic to Lower Cretaceous synorogenic sedimentary rocks in the southern Spring Mountains, Nevada: *Geology*, v. 8, no. 8, p. 385-389.
- , 1983, Geometry and structural history of the Mesozoic thrust belt in the Goodsprings District, southern Spring Mountains, Nevada: Geological Society of America Bulletin, v. 94, no. 10, p. 1185-1198.
- Carr, M.D., and Pinkston, J.C., 1987, Geologic map of the Goodsprings District, southern Spring Mountains, Clark County, Nevada: U.S. Geological Survey Miscellaneous Field Studies Map MF-1514, 1 sheet, 1:24,000 scale.
- Christenson, G.E., and Purcell, C., 1985, Correlation and age of Quaternary alluvial-fan sequences, Basin and Range province, southwestern United States, *in* Weide, D.L., ed., Soils and Quaternary geology of the southwestern United States: Geological Society of America Special Paper 203: Denver, CO, p. 115-122.
- Clary, M., 1967, Geology of the eastern part of the Clark Mountain Range, San Bernardino County, California, California Division of Mines and Geology, Map Sheet, v. 67, no. 6, 1:24,000 scale.
- Cooke, R.U., 1970, Stone pavements in deserts: *Annals of the Association of American Geographers*, v. 60, no. 3, p. 560-577.
- Cunningham, G.L., Sylversten, J.P., Reynolds, J.F., and Wilson, J.M., 1979, Some effects of soil-moisture availability on above-ground production and reproduction allocation in *Larrea tridentata* (DC) cov.: *Oecologia*, v. 40, p. 113-123.
- Czarnecki, J.B., 1990, Geohydrology and evapotranspiration at Franklin Lake playa, Inyo County, California: U. S. Geological Survey Open-File Report 90-035. 96 p.
- Davis, G.A., Fowler, T.K., Bishop, K.M., Brudos, T.C., Friedmann, S.J., Burbank, D.W., Parke, M.A., and Burchfiel, B.C., 1993, Pluton pinning of an active Miocene detachment fault system, eastern Mojave Desert, California: *Geology*, v. 21, p. 627-630.
- Denny, C.S., 1965, Alluvial fans in the Death Valley region, California and Nevada: U.S. Geological Survey Professional Paper 466, 66 p.
- DeWitt, E., Anderson, J.L., Barton, H.N., Jachens, R.C., Podwysoki, M.H., Brickey, D.W., and Close, T.J., 1989, Mineral resources of the south McCullough Mountains wilderness study area, Clark County, Nevada: U.S. Geological Survey Bulletin 1730-C, 24 p.
- Dokka, R.K., 1989, The Mojave extensional belt of California: *Tectonics*, v. 8, p. 363-390.

- Dokka, R.K., and Travis, C.J., 1990, Late Cenozoic strike-slip faulting in the Mojave Desert, California: *Tectonics*, v. 9, no. 2, p. 311-340.
- Faulds, J.E., Smith, E.I., and Gans, P., 1999, Spatial and temporal patterns of magmatism and extension in the northern Colorado River extensional corridor, Nevada and Arizona: A preliminary report: *Nevada Petroleum Society Guidebook*, p. 171-183.
- Faulds, J.E., Olson, E.L., Harlan, S.S., and McIntosh, W.C., 2002, Miocene extension and fault-related folding in the Highland Range, southern Nevada: a three-dimensional perspective: *Journal of Structural Geology*, v. 24, no. 4, p. 861-886.
- Field, J.J., and Pearthree, P.A., 1997, Geomorphic flood-hazard assessment of alluvial fans and piedmonts: *Journal of Geoscience Education*, v. 45, p. 27-37.
- Fleck, R.J., 1970, Tectonic style, magnitude, and age of deformation in the Sevier orogenic belt in southern Nevada and eastern California: *Geological Society of America Bulletin*, v. 81, no. 6, p. 1705-1720.
- Fleck, R.J., and Carr, M.D., 1990, The age of the Keystone Thrust; laser-fusion $^{40}\text{Ar}/^{39}\text{Ar}$ dating of foreland basin deposits, southern Spring Mountains, Nevada: *Tectonics*, v. 9, no. 3, p. 467-476.
- Fleck, R.J., Mattinson, J.M., Busby, C.J., Carr, M.D., Davis, G.A., and Burchfiel, B.C., 1994, Isotopic complexities and the age of the Delfonte volcanic rocks, eastern Mescal Range, southeastern California; stratigraphic and tectonic implications: *Geological Society of America Bulletin*, v. 106, no. 10, p. 1242-1253.
- Forester, R.M., Bradbury, J.P., Carter, C., Elvidge-Tuma, A.B., Hemphill, M.L., Lundstrum, S.C., Mahan, S.A., Marshall, B.D., Neymark, L.A., Paces, J.B., Sharpe, S.E., Whelan, J.F., and Wigand, P.E., 1999, The climatic and hydrologic history of southern Nevada during the late Quaternary: U.S. Geological Survey Open-File Report 98-0635, 63 p.
- Fowler Jr., T.K., and Calzia, J.P., 1999, Kingston Range detachment fault, southeastern Death Valley, California: relation to Tertiary deposits and reconstruction of initial dip, *in* Wright, L.A., and Troxel, B.W., eds., *Cenozoic basins of the Death Valley region*: Boulder, Colorado, Geological Society of America Special Paper 333, p. 245-257.
- French, R.H., 1983, Precipitation in southern Nevada: *Journal of Hydraulic Engineering*, v. 109, no. 7, p. 1023-1036.
- Friedmann, J.S., Davis, G.A., and Fowler, T.K., 1996, Geometry, paleodrainage, and geologic rates from the Miocene Shadow Valley supradetachment basin, eastern Mojave Desert, California, *in* Beratan, K.K., ed., *Reconstructing the history of Basin and Range extension using sedimentology and stratigraphy*, Geological Society of America Special Paper 303, p. 85-105.
- Friedmann, S.J., 1999, Sedimentology and stratigraphy of the Shadow Valley basin, eastern Mojave Desert, California, *in* Wright, L.A., and Troxel, B.W., eds., *Cenozoic basins of the Death Valley region*: Boulder, Colorado, Geological Society of America Special Paper 333, p. 213-243.
- Gianella, V.P., and Callaghan, E., 1934, The earthquake of December 20, 1932 at Cedar Mountain, Nevada, and its bearing on the genesis of Basin Range structure: *Journal of Geology*, v. 42, p. 1-22.
- Gile, L.H., Peterson, F.F., and Grossman, R.B., 1965, The K horizon- A master soil horizon of carbonate accumulation: *Soil Science*, v. 99, p. 74-82.
- , 1966, Morphological and genetic sequences of carbonate accumulation in desert soils: *Soil Science*, v. 101, p. 347-360.
- Glazner, A.F., Walker, J.D., Bartley, J.M., and Fletcher, J.M., 2002, Cenozoic evolution of the Mojave Block of Southern California, *in* Glazner, A.F., Walker, J.D., and Bartley, J.M., eds.,

- Geologic evolution of the Mojave Desert and southwestern Basin and Range, Geological Society of America Memoir 195, p. 19-41.
- Hammerlynck, E.P., McAuliffe, J.R., McDonald, E.V., and Smith, S.D., 2002, Ecological responses of two Mojave Desert shrubs to soil horizon development and soil water dynamics: *Ecology*, v. 83, no. 3, p. 768-779.
- Hewett, D.F., 1931, Geology and ore deposits of the Goodsprings quadrangle, Nevada: U.S. Geological Survey Professional Paper 162, 172 p.
- , 1956, Geology and mineral resources of the Ivanpah Quadrangle California and Nevada: U.S. Geological Survey Professional Paper 275, 172 p.
- Hill, J.M., 1914, The Yellow Pine mining district, Clark County, Nevada: U.S. Geological Survey Bulletin 540, p. 223-274.
- Hoffard, J.L., 1991, Quaternary tectonics and basin history of Pahrump and Stewart Valleys, Nevada and California: Reno, N.V., University of Nevada, Reno, M.S., 138 p.
- House, P.K., and Park, B.K., 2003, Preliminary Quaternary geologic map of the east half of the Goodsprings quadrangle, Clark County, Nevada: Nevada Bureau of Mines and Geology Open-File Report 03-24, scale 1:24,000.
- House, P.K., 2004, Preliminary Quaternary geologic map of the Jean quadrangle, Clark County, Nevada: Nevada Bureau of Mines and Geology Open-File Report 03-23, scale 1:24,000.
- House, P.K., Park, B.K., and Ramelli, A.R., 2004, Preliminary surficial geologic map of the Nevada part of the Desert quadrangle, Clark County, Nevada: Nevada Bureau of Mines and Geology Open-File Report 04-05, scale 1:24,000.
- Izbicki, J.A., Radyk, J., and Michel, R.L., 2000, Water movement through a thick unsaturated zone underlying an intermittent stream in the western Mojave Desert, southern California, USA: *Journal of Hydrology*, v. 238, p. 194-217.
- Jennings, C.W., Burnett, J.L., and Troxel, B.W., 1962, Geologic map of California, Olaf P. Jenkins edition; Trona sheet, California Division of Mines and Geology, 1:250,000 scale.
- Johansen, J., 1993, Cryptogamic crusts of semi-arid and arid lands of North America: *Journal of Phycology*, v. 29, p. 146-147.
- Jones, C.H., Wernicke, B.P., Farmer, G.L., Walker, J.D., Coleman, D.S., McKenna, L.W., and Perry, F.V., 1992, Variations across and along a major continental rift; an interdisciplinary study of the Basin and Range Province, Western USA: *Tectonophysics*, v. 213, no. 1-2, p. 57-96.
- Kaufman, P.S., and Royden, L.H., 1994, Lower crustal flow in an extensional setting; constraints from the Halloran Hills region, eastern Mojave Desert, California: *Journal of Geophysical Research*, B, Solid Earth and Planets, v. 99, no. 8, p. 15,723-15,739.
- Koehler, P.A., Anderson, R.S., and Spaulding, W.G., 2005, Development of vegetation in the central Mojave Desert of California during the late Quaternary: *Palaeogeography, Palaeoclimatology, Palaeoecology*, v. 215, no. 3-4, p. 297-311.
- Langenheim, V.E., Grow, J.A., Jachens, R.C., Dixon, G.L., and Miller, J.J., 2001, Geophysical constraints on the location and geometry of the Las Vegas Valley shear zone, Nevada: *Tectonics*, v. 20, no. 2, p. 189-209.
- Langer, A.M., 1965, Mineralogy and physical properties of Mojave Desert (California) playa crusts: Palisades, NY, United States (USA), Columbia University, Unpublished doctoral dissertation.
- Langer, A.M., and Kerr, P.F., 1966, Mojave playa crusts: physical properties and mineral content: *Journal of Sedimentary Petrology*, v. 36, p. 377-396.

- Lattman, L.H., 1973, Calcium carbonate cementation of alluvial fans in southern Nevada: *Geological Society of America Bulletin*, v. 84, p. 3013-3028.
- , 1977, Weathering of caliche in southern Nevada, *in* A proceedings volume of the annual geomorphology symposia series, no. 8, Fort Collins, CO, State University of New York, Binghamton, NY, p. 221-231.
- Lattman, L.H., and Simonberg, E.M., 1971, Case-hardening of carbonate alluvium and colluvium, Spring Mountains, Nevada: *Journal of Sedimentary Petrology*, v. 41, no. 1, p. 274-281.
- Liu, T., and Broecker, W.S., 2000, How fast does rock varnish grow?: *Geology*, v. 28, no. 2, p. 183-186.
- Longwell, C.R., 1960, Possible explanation of diverse structural patterns in southern Nevada: *American Journal of Science*, v. 258-A, p. 192-203.
- Longwell, C.R., Pampeyan, E.H., Bowyer, B., and Roberts, R.J., 1965, Geology and mineral deposits of Clark County, Nevada: *Nevada Bureau of Mines and Geology Bulletin* 62, 218 p.
- Louie, J., Shields, G., Ichinose, G.A., Hastings, M., Plank, G., and Bowman, S., 1998, Shallow geophysical constraints on displacement and segmentation of the Pahrump Valley fault zone, California-Nevada border: *Miscellaneous Publication - Utah Geological Survey*, v. 98-2, p. 139-146.
- Lundstrom, S.C., Mahan, S.A., Blakely, R.J., Paces, J.B., Young, O.D., Workman, J.B., and Dixon, G.L., 2003, Geologic map of the Mound Spring quadrangle, Nye and Clark Counties, Nevada, and Inyo County, California: *U.S. Geological Survey Miscellaneous Field Studies Map MF-2339*, 1:24,000 scale, 8 p.
- Machette, M.N., 1985, Calcic soils of the southwestern United States, *in* Weide, D.L., ed., *Soils and Quaternary geology of the southwestern United States: Geological Society of America Special Paper 203*: Denver, CO, p. 1-21.
- Malmberg, G.T., 1967, Hydrology of the valley-fill and carbonate-rock reservoirs, Pahrump Valley, Nevada-California: *U.S. Geological Survey Water-Supply Paper* 1832, 47 p.
- Maxey, G.B., and Robinson, T.W., 1947, Ground water in Las Vegas, Pahrump, and Indian Spring Valleys, Nevada: *U.S. Geological Survey Water Resources Bulletin* No. 6, 23 p.
- McAuliffe, J.R., 1994, Landscape evolution, soil formation, and ecological patterns and processes in Sonoran desert bajadas: *Ecological Monographs*, v. 64, no. 2, p. 111-148.
- McAuliffe, J.R., and McDonald, E.V., 1995, A piedmont landscape in the eastern Mojave Desert; examples of linkages between biotic and physical components: *Quarterly of San Bernardino County Museum Association*, v. 42, no. 3, p. 53-63.
- McDonald, E.V., 1994, The relative influences of climatic change, desert dust, and lithologic control on soil-geomorphic processes and soil hydrology of calcic soils formed on Quaternary alluvial-fan deposits in the Mojave Desert, California, *University of New Mexico, Unpublished Doctoral Dissertation*, 382 p.
- McDonald, E.V., McFadden, L.D., and Wells, S.G., 2003, Regional response of alluvial fans to the Pleistocene-Holocene climatic transition, Mojave Desert, California, *in* Enzel, Y., Wells, S.G., and Lancaster, N., eds., *Paleoenvironments and paleohydrology of the Mojave and southern Great Basin Deserts*: Boulder, Colorado, *Geological Society of America Special Paper* 368, p. 189-205.
- McDonald, E.V., Pierson, F.B., Flerchinger, G.N., and McFadden, L.D., 1996, Application of a soil-water balance model to evaluate the influence of Holocene climate change on calcic soils, Mojave Desert, California, U.S.A.: *Geoderma*, v. 74, p. 167-192.

- McFadden, L.D., McDonald, E.V., Wells, S.G., Anderson, K., Quade, J., and Forman, S.L., 1998, The vesicular layer and carbonate collars of desert soils and pavements: formation, age and relation to climate change: *Geomorphology*, v. 24, p. 101-145.
- McFadden, L.D., Ritter, J.B., and Wells, S.G., 1989, Use of multiparameter relative-age methods for age estimation and correlation of alluvial fan surfaces on a desert piedmont, eastern Mojave Desert, California: *Quaternary Research*, v. 32, p. 276-290.
- McFadden, L.D., Wells, S.G., and Dohrenwend, J.C., 1986, Influences of Quaternary climatic changes on processes of soil development on desert loess deposits of the Cima volcanic field, California: *Catena*, v. 13, p. 361-389.
- McFadden, L.D., Wells, S.G., and Jercinovich, M.J., 1987, Influences of eolian and pedogenic processes on the origin and evolution of desert pavements: *Geology*, v. 15, p. 504-508.
- McMackin, M.R., 1988, Cenozoic sedimentation and tectonics of the Kingston Range, *in* Weide, D.L., and Faber, M.L., eds., *This extended land: geological excursions in the southern Basin and Range: Las Vegas, University of Nevada, Department of Geosciences*, p. 221-222.
- , 1992, Tectonic evolution of the Kingston Range, Death Valley, California: University Park, Pennsylvania, Pennsylvania State University, unpublished doctoral dissertation, 158 p.
- , 1999, Geology of the Stump Spring quadrangle— Evidence of Late Quaternary transpression on the southern segment of the Pahrump Valley fault zone, Nevada and California, *in* *Proceedings on the Status of Geologic Research and Mapping in Death Valley National Park, Las Vegas, Nevada, U.S. Geological Survey Open-File Report 99-153*, p. 162.
- Motts, W.S., 1965, Hydrologic types of playas and closed valleys and some relation of hydrology to playa geology, *in* Neal, J.T., ed., *Geology, mineralogy, and hydrology of U.S. Playas: Bedford Massachusetts, Air Force Research Laboratory Environmental Research Papers v. 96*, p. 73-105.
- NRCS, 1997, Introduction to microbiotic crusts: Natural Resources Conservation Service, United States Department of Agriculture, Soil Quality – Soil Biology Technical Note No. 2, 13 p.
- Page, W.R., Lundstrum, S.C., Harris, A.G., Langenheim, V.E., Workman, J.B., Mahan, S.A., Paces, J.B., Dixon, G.L., Rowley, P.D., Burchfiel, B.C., Bell, J.W., and Smith, E.I., 2005, Geologic and geophysical maps of the Las Vegas 30' X 60' quadrangle, Clark and Nye Counties, Nevada, and Inyo County, California: U.S. Geological Survey Scientific Investigations Map 2814, scale 1:100,000, 55 p.
- Peterson, F.F., 1981, Landforms of the Basin and Range Province defined for soil survey: University of Nevada, Nevada Agricultural Experiment Station Technical Bulletin 28, 52 p.
- Prave, A.R., and McMackin, M.R., 1999, Depositional framework of mid- to late Miocene strata, Dumont Hills and southern margin Kingston Range: Implications for the tectonostratigraphic evolution of the southern Death Valley region, *in* Wright, L.A., and Troxel, B.W., eds., *Cenozoic basins of the Death Valley region: Boulder, Colorado, Geological Society of America Special Paper 333*, p. 259-275.
- Quade, J., Forester, R.M., and Whelan, J.F., 2003, Late Quaternary paleohydrologic and paleotemperature change in southern Nevada, *Geological Society of America Special Paper 368*, p. 165-188.
- Quade, J., Mifflin, M.D., Pratt, W.L., McCoy, W., and Burckle, L., 1995, Fossil spring deposits in the southern Great Basin and their implications for changes in water-table levels near Yucca Mountain, Nevada, during Quaternary time: *Geological Society of America Bulletin*, v. 107, p. 213-230.

- Ramelli, A.R., Park, B.K., and House, P.K., 2003, Preliminary Quaternary geologic map of the east half of the State Line Pass quadrangle, Clark County, Nevada, San Bernardino County, California: Nevada Bureau of Mines and Geology Open-File Report 03-26, scale 1:24,000.
- , 2004a, Preliminary surficial geologic map of the Roach quadrangle, Clark County, Nevada: Nevada Bureau of Mines and Geology Open-File Report 04-07, scale 1:24,000.
- , 2004b, Preliminary surficial geologic map of the west half of the McCullough Pass quadrangle, Clark County, Nevada: Nevada Bureau of Mines and Geology Open-File Report 04-06, scale 1:24,000.
- Reheis, M.C., Harden, J.W., McFadden, L.D., and Shroba, R.R., 1989, Development rates of late Quaternary soils, Silver Lake Playa, California: *Soil Science Society of America Journal*, v. 53, p. 1127-1140.
- Reheis, M.C., Slate, J.L., Throckmorton, C.K., McGeehin, J.P., Sarna-Wojcicki, A.M., and Dengler, L., 1996, Late Quaternary sedimentation on the Leidy Creek fan, Nevada-California: geomorphic responses to climate change: *Basin Research*, v. 12, p. 279-299.
- Rosen, M.R., 1994, The importance of groundwater in playas: A review of playa classifications and the sedimentology and hydrology of playas, *in* Rosen, M.R., ed., *Paleoclimate and basin evolution of playa systems: Boulder, Colorado*, Geological Society of America Special Paper 289, p. 1-18.
- Schlesinger, W.H., Fonteyn, P.J., and Reiners, W.A., 1989, Effects of overland flow on plant water relations, erosion, and soil water percolation on a Mojave Desert landscape: *Soil Science Society of America Journal*, v. 53, p. 1567-1572.
- Schmidt, K.M., and Menges, C.M., 2003, Debris-flow deposits and watershed erosion rates near southern Death Valley, CA, United States, *in* Rickenmann, D., and Chen, C., eds., *Debris-flow hazards mitigation: mechanics, prediction, and assessment: Davos, Switzerland*, Millpress, p. 219-230.
- Sharifi, M.R., Meinzer, F.G., Nilsen, E.T., Rundel, P.W., Virginia, R.A., Jarrell, W.M., Herman, D.J., and Clark, P.C., 1988, Effect of manipulation of water and nitrogen supplies on the quantitative phenology of *Larrea tridentata* (creosote bush) in the Sonoran Desert of California: *American Journal of Botany*, v. 75, no. 8, p. 1163-1174.
- Shreve, F., and Mallery, T.D., 1933, The relationship of caliche to desert plants: *Soil Science*, v. 35, p. 99-113.
- Spaulding, W.G., 1990, Vegetational and climatic development of the Mojave Desert-The last glacial maximum to the present, *in* Betancourt, J.L., Van Devender, T.R., and Martin, P.S., eds., *Fossil packrat middens-The last 40,000 years of biotic change: Tucson, AZ*, University of Arizona Press, p. 166-199.
- Steiger, J.W., and Webb, R.H., 2000, Recovery of perennial vegetation in military target sites in the eastern Mojave Desert, Arizona: U.S. Geological Survey Open-File Report 00-0355, 28 p.
- Stevens, C.H., Stone, P., and Belasky, P., 1991, Paleogeographic and structural significance of an Upper Mississippian facies boundary in southern Nevada and east-central California; with Suppl. Data 91-14: *Geological Society of America Bulletin*, v. 103, no. 7, p. 876-885.
- Stock, J.D., Schmidt, K.M., and Miller, D.M., 2004, Observations on alluvial fans with relevance to recent sediment transport: *Eos Transactions*, v. 85, no. 47, p. abstract #H41G-03.
- Topping, D.J., 1993, Paleogeographic reconstruction of the Death Valley extended region: evidence from Miocene large rock-avalanche deposits in the Amargosa Chaos basin, California: *Geological Society of America Bulletin*, v. 105, p. 1190-1213.

- Turner, R.L., 1990, Analytical data for stream and playa sediment samples from the Kingman 1° by 2° quadrangle, Arizona, California and Nevada: U.S. Geological Survey Open-File Report 90-444, 2 computer disks; 5 1/4 in.
- Walker, J.D., Burchfiel, B.C., and Davis, G.A., 1995, New age controls on initiation and timing of foreland belt thrusting in the Clark Mountains, Southern California: Geological Society of America Bulletin, v. 107, no. 6, p. 742-750.
- Webb, R.H., Steiger, J.W., and Newman, E.B., 1988, The effects of disturbance on desert vegetation in Death Valley National Monument, California: U.S. Geological Survey Bulletin 1793, 103 p.
- Webb, R.H., Steiger, J.W., and Turner, R.M., 1987, Dynamics of Mojave desert shrub assemblages in the Panamint Mountains, California: Ecology, v. 68, no. 3, p. 478-490.
- Wells, S.G., Dohrenwend, J.C., McFadden, L.D., Turrin, B.D., and Mahrer, K.D., 1985, Late Cenozoic landscape evolution on lava flow surfaces of the Cima volcanic field, Mojave Desert, California: Geological Society of America Bulletin, v. 96, p. 1518-1529.
- Wells, S.G., and McFadden, L.D., 1987, Influence of Late Quaternary climatic changes on geomorphic and pedogenic processes on a desert piedmont, Eastern Mojave Desert, California: Quaternary Research, v. 27, p. 130-146.
- Wernicke, B.R., Axen, G.J., and Snow, J., 1988, Basin and Range extensional tectonics at the latitude of Las Vegas, Nevada: Geological Society of America Bulletin, v. 100, p. 1738-1757.
- Whitney, J.W., and Harrington, C.D., 1993, Relict colluvial boulder deposits as paleoclimatic indicators in the Yucca Mountain region, southern Nevada: Geological Society of America Bulletin, v. 105, p. 1008-1018.
- Wright, L.A., 1968, Talc deposits of the southern Death Valley- Kingston Range region, California: California Division of Mines and Geology Special Report 95, p. 1-79.
- Wright, L.A., Stewart, R.M., Gay, T.E., Jr., and Hazenbush, G.C., 1953, Mines and mineral deposits of San Bernardino County, California: California Journal of Mines and Geology, v. 49, no. 1 and 2, 451 p.
- Yount, J.C., Schermer, E.R., Felger, T.J., Miller, D.M., and Stephens, K.A., 1994, Preliminary geologic map of Fort Irwin Basin, north-central Mojave Desert, California, U.S. Geological Survey Open-File Report 94-173, 1:24,000 scale, 27 p.

Figures

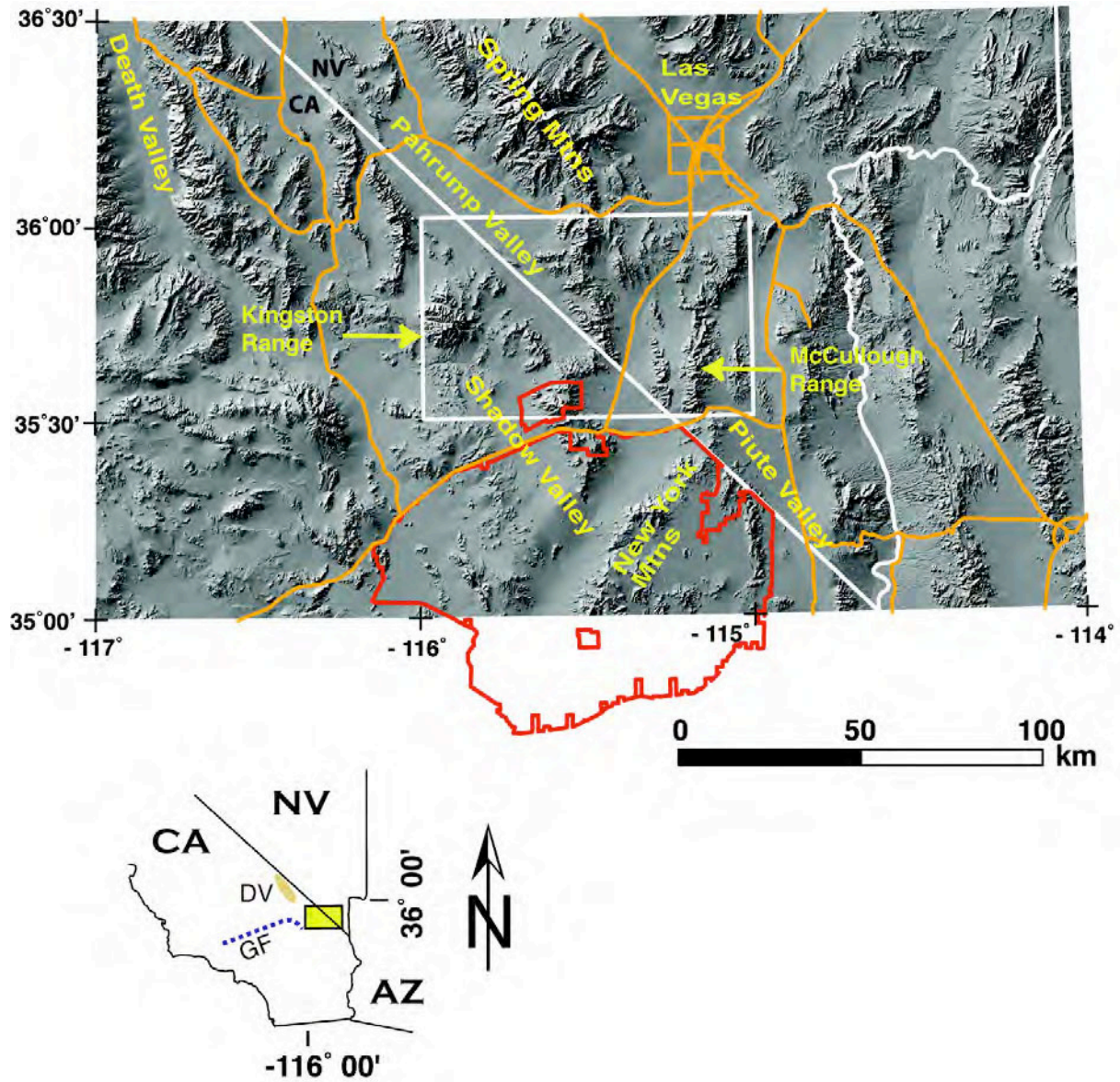


Figure 1. Regional topography in hillshade of study area with 30' X 60' Mesquite Lake quadrangle boundary shown as white rectangle. Roads are depicted in orange, major valleys labeled in yellow, California, Nevada, and Arizona state lines as white lines, and Mojave National Preserve boundary in red. The state line separates San Bernardino and Inyo Counties in California from Clark County in Nevada.

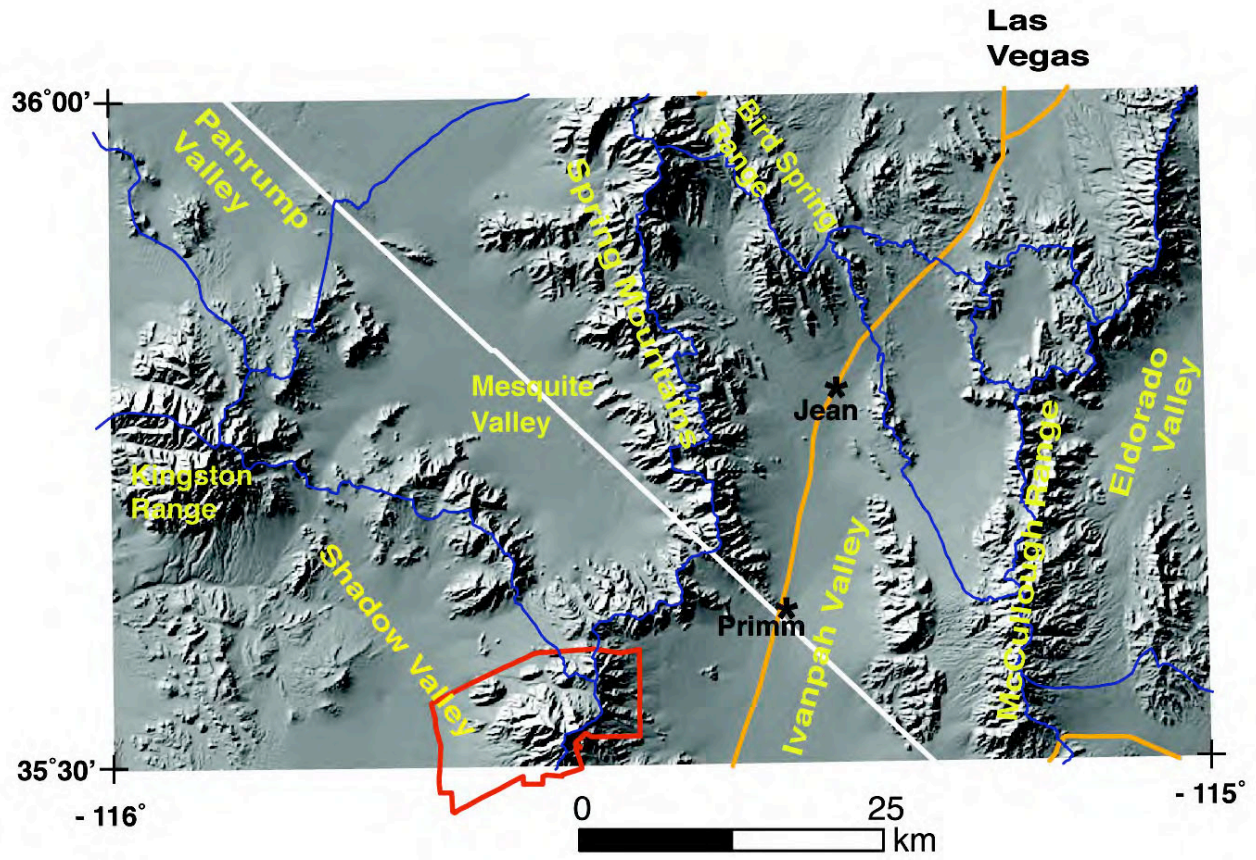


Figure 2. Hillshade topography of Mesquite Lake 30' X 60' Mesquite Lake quadrangle showing principal geographic features in yellow, main roads in orange, primary drainage divides in blue, the California-Nevada state line in white, and the Mojave National Preserve in red.

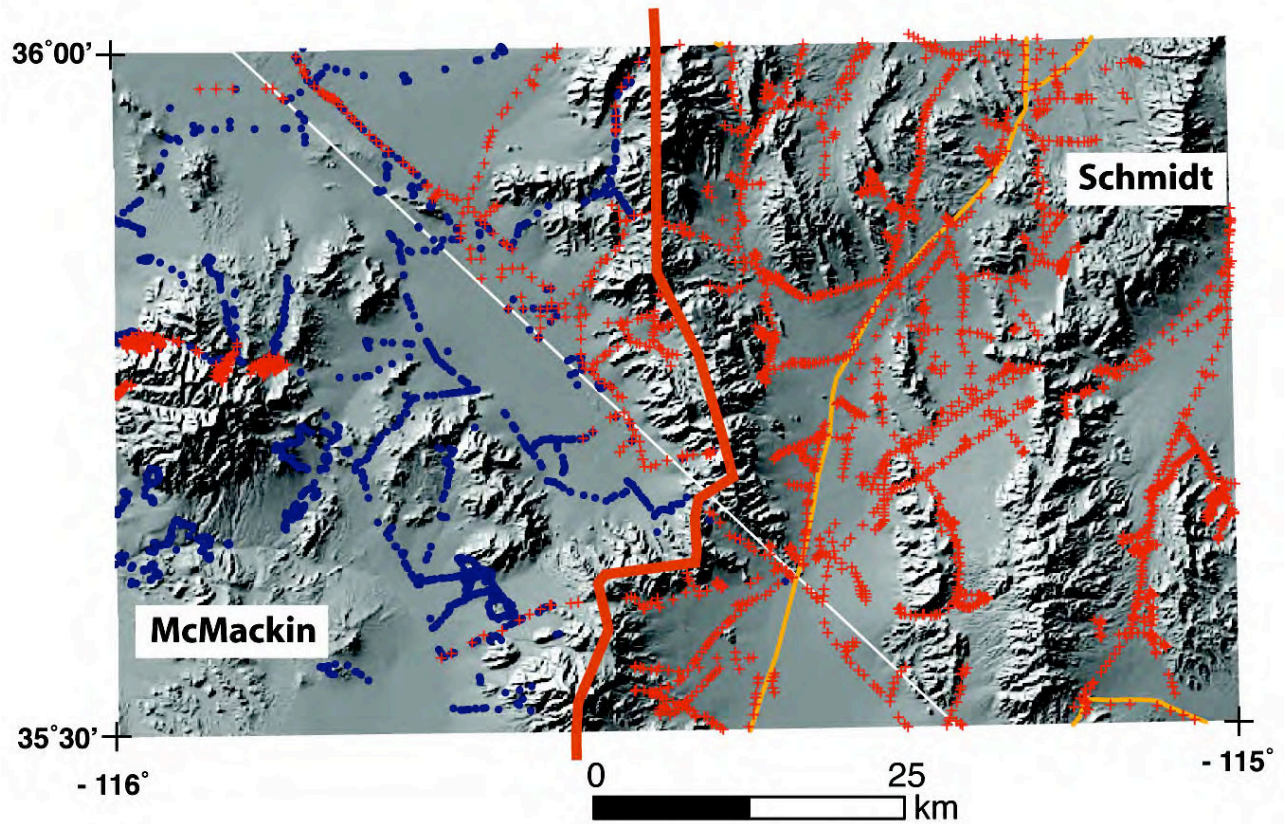


Figure 3. Authorship boundaries of mapping extent within 30' X 60' Mesquite Lake quadrangle. Orange line separates authorship with GPS waypoints collected by McMackin as blue dots and by Schmidt as red crosses. Stateline included as reference white line.



Figure 4. View ~ 250° of Qoa (~6 m thick) overlying carbonate and siliciclastic bedrock (reddish sandstone) in middleground and the southern Bird Spring Range in background.



Figure 5. View approximately south of exposed (Qhs) and colluvially mantled (Qha) Kingston Peak Formation granite near Tecopa Pass in the Kingston Range.



Figure 6. Mid Holocene aged deposit composed of equigranular grus dominated by potassium feldspar overlying silty sandy A horizon largely devoid of vesicles. Ruler with color scale on whiteboard is ~ 10 cm long.



Figure 7. Active boulders deposited by debris-flow processes under dashboard and steering column of abandoned vehicle east of Tecopa Pass in Kingston Range.

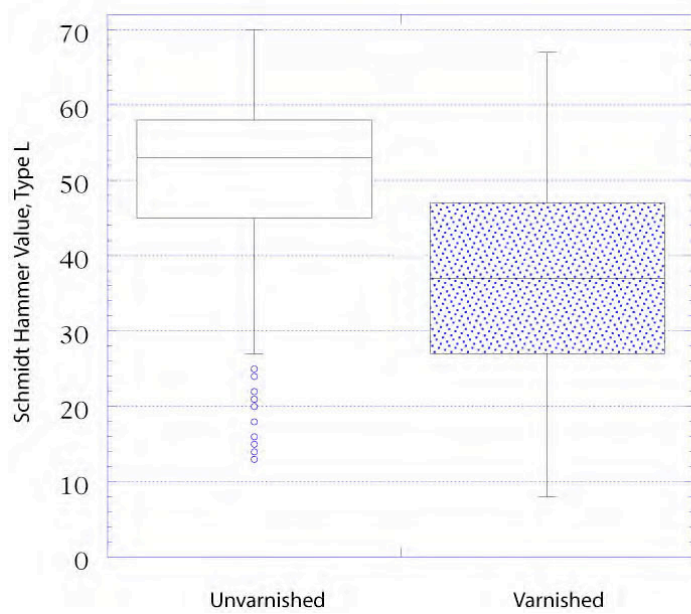
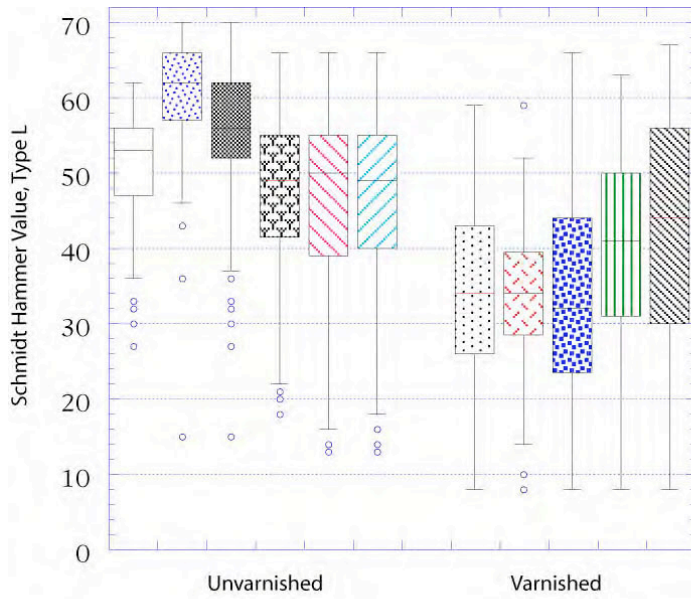


Figure 8. Schmidt Hammer Values of Kingston Peak granite depicting decrease in strength of surface hardness as initially unvarnished outcrops become varnished and weather to grus. Upper plot depicts all measured sites separately while lower plot depicts averaged values for younger unvarnished and older varnished outcrops. Each vertically oriented rectangle encloses 50% of the data with the median value of the variable displayed as a horizontal line and the top (upper quartile) and bottom of the box (lower quartile) mark the interquartile distance.



Figure 9. View approximately south of a balanced boulder as evidence for debris-flow transport in proximal fan within Kingston Range, near Crystal Spring.



Figure 10. Pronounced chemical weathering of calcium carbonate clast forming solution cavities at surface of Qoa deposit, note 6 inch (15 cm) clear ruler for scale left of notebook. Effective surface lowering measured between solution cavity depths roughly parallel to present deposit surface and highest point on boulder is ~ 8 cm.



Figure 11. Roughly planar stage IV B_{km} horizon exposed at surface and covered by thin disaggregated pavement of Qoa deposit. Note 15 cm long hand-held GPS unit for scale.



Figure 12. Mid Pleistocene alluvial deposit (Qia) composed of carbonate bedrock clasts overlying silty A_v horizon ~ 7 cm thick. Note relative lack of desert varnish on moderately interlocking pavement clasts.



Figure 13. View to the south showing the northwest Kingston Range piedmont with a late Pleistocene alluvium (Qia) veneer over stage IV carbonate-cemented B_{km} horizon from older alluvium.



Figure 14. Moderately varnished mid Pleistocene (Qia) pavement composed primarily of carbonate clasts with minor volcanic clasts. Note prismatic soil structure of A_v ped to right of shallow soil pit with knife in shadow.



Figure 15. Mid Holocene age alluvial deposit composed of randomly structured calcium carbonate bedrock clasts overlying sandy, silty, loose and unstructured A horizon. The unit potentially represents increased eolian fine material derived from nearby Roach Lake playa.



Figure 16. View west in Kingston Wash of active channel (Qaa) inset within Qia/pc deposit.



Figure 17. View roughly north of small active channel (Qaag) inset within Qiag deposit near Colosseum Gorge northeast of Clark Mtn. Note reddish brown B_w horizon and stage III B_{km} horizon in Qiag.



Figure 18. View along northbound direction of Interstate 15 traffic heading into dust storm on Ivanpah and Roach Lake playas on April 15, 2002 with Primm, Nevada in background.



Figure 19. View 260° of active sand ramps climbing onto basalt (Qaer/mv) of McCollough Range near Hidden Valley. Foreground units dominated by young alluvium (Qya) and mixed eolian-alluvial deposits (Qyea).



Figure 20. View northwest from Stateline Pass of active dust storm on Mesquite Lake playa.



Figure 21. View north of deflated sand dunes on east edge of Mesquite Lake playa. Note Qia soil exposed at base of mesquite topped dunes. Eolian deflation has lowered surface exposing gypsiferous playa sediments in lower left side marked by *Atriplex*.



Figure 22. View northwest of Roach Lake playa, Interstate 15, and the southern Spring Mountains on March 21, 2001 with shallow standing water over typically dry playa surface (Qap).



Figure 23. View southeast of active dust storm from Roach Lake playa on March 25, 2001 with Lucy Gray Mountains and McCullough Range in background. Note, photograph of dust storm was taken four days after water observed on playa surface making roads across the playa surface impassable (fig. 20).



Figure 24. Gypsum-rich sediment exposed by deflation of Mesquite Lake bed. Elongate crystalline gypsum is overlain by progressively thicker, horizontal laminated mud toward the seasonal wetland on the floor of active Mesquite Valley wet playa sediment (Qapw).



Figure 25. Bed of crystalline gypsum of the crystal body playa unit in Mesquite Lake Valley. In this view the upper bed, about 1 meter, is composed of approximately 60% intergrown gypsum crystals and 40% mud. Such crystal bed typically form below the surface and in this case are exposed in the uplifted of a fault transects the Mesquite Lake Basin (J, fig. 28).



Figure 26. Young playa fringe deposit (Qypf) on the west side of the Mesquite Lake Basin with a buried soil overlain by alluvial sand of a distal fan from the Mesquite Mountains. The whole section is cemented with gypsum precipitated by ground water discharge.

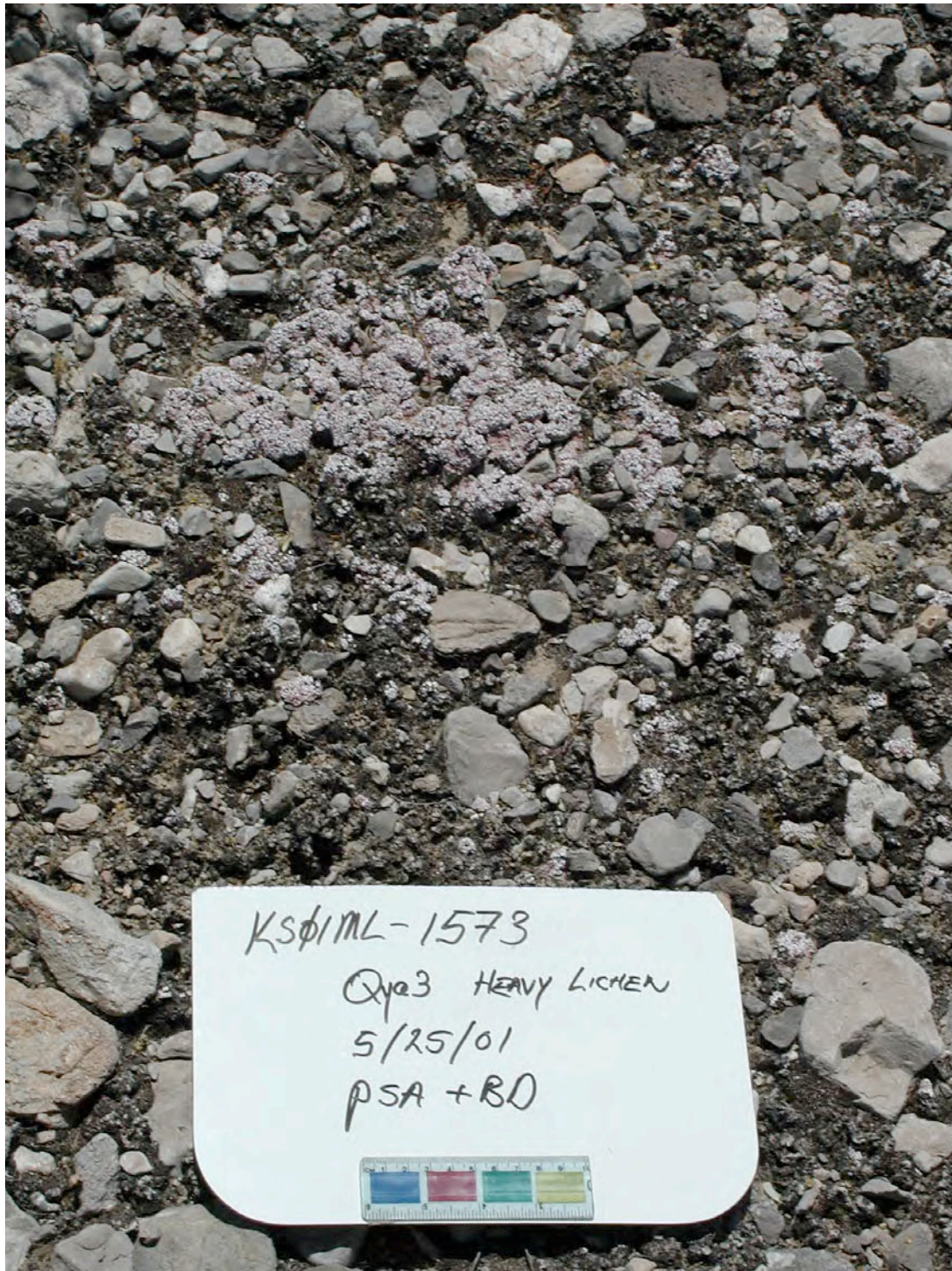


Figure 27. Mid Holocene deposit (Qya3) with heavy lichen cover with black, dark brown, and pinkish color. Clasts dominated by carbonate with some volcanic source rock.

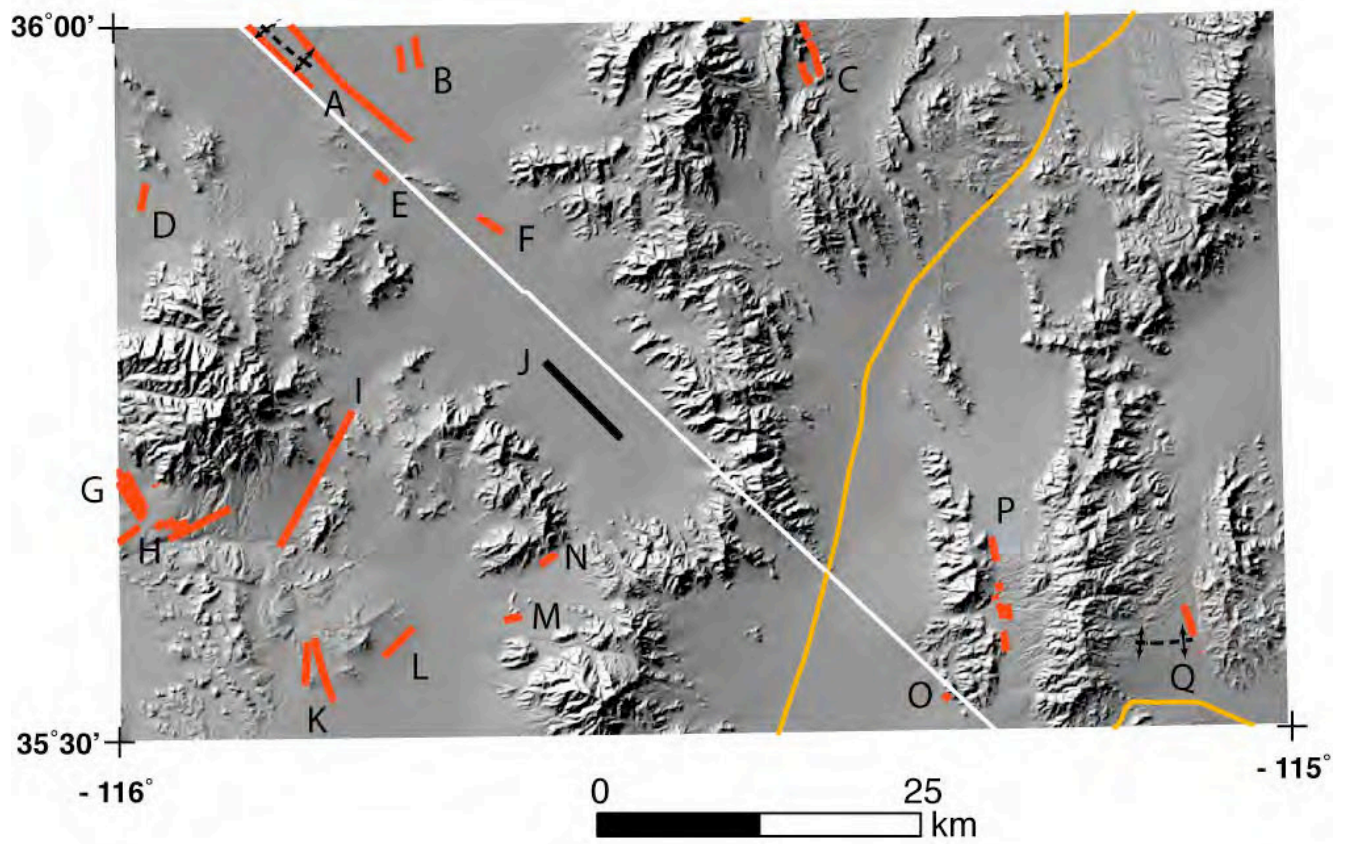


Figure 28. Hillshade topography depicting faults, lineaments, and folds presented in the map on plate 1 and table 1. Faults in red, lineaments in black, and fold axes in dashed black line.



Figure 29. Truncated Qoa deposit (middle ground) with ~ 2 m of projected separation above Qia deposit (foreground). Note, break in slope at potential fault location also corresponds to only a 1 m separation between different bedrock types (ca and sl) exposed in channel cuts.



a)



b)

Figure 30. (A) Southeast oriented regional view of topographically back-facing talus slopes (Qoa in age) and broad topographic saddle in bedrock of Bird Spring Range. (B) Southeast oriented close-up view of topographically back-facing talus slopes (Qoa in age). Source region for talus slopes is currently separated by subtle topographic depression.



Figure 31. Fault cutting older Quaternary sand deposits (Qoe) exposed in side canyon of Kingston Wash near Coyote Holes Spring. One meter tall boy for scale.



Figure 32. Carbonate-cemented faults cutting older Quaternary alluvium (Qoa) overlain by ~ 1 m of unfaulted mid and late Pleistocene (Qia) alluvial deposits. One of many faults exposed in a zone straddling the north fork of Kingston Wash (I, fig. 28). One-half meter tall meter dog stands on a Qia surface for scale.

Tables

Table 1. Characteristics of tectonic features, faults, folds, and lineaments, depicted in map on plate 1 and fig. 28.

Fault ID	Reliability of location	Length (km)	Average strike	Geomorphic expression	Sense of movement	Age of youngest faulted deposit
A	Approximately located and concealed	> 7 - 13	N45°W	Valley axis, intrabasin	Dextral and vertical, up to the east	Qiv?
B	Approximately located and concealed	2 - 2.5	N10°W	Distal fan	Normal, up to the east	Qov
C	Queried	1.6 – 4.4	~N20°W	Mountain front and proximal fan	Normal?	Qoa
D	Approximately located, concealed, and queried	2.2	N10°E	Distal fan	Normal, down to the west. Sinistral oblique?	Qoa
E	Concealed	1.3	N50°W	Valley axis, intrabasin	Normal, down to the west	Qig
F	Approximately located and concealed	2.4	N55°W	Valley axis, intrabasin	Normal, down to the west. Dextral oblique?	Qig
G	Certain, approximately located, concealed, and queried	3.3 – 4.2	N30°W	Proximal fan	Dextral	Qiea
H	Certain, approximately located, concealed, and queried	0.8 - 5.3	N50-65°E	Mid to distal fan	Normal, reverse, and strike slip	Qiea
I	Certain, approximately located, and concealed	12	N30°E	Valley axis, intrabasin	Multiple faults in a zone. Normal and sinistral?	Qoa
J	Approximately located lineament	8.4	N45°W	Valley axis, intrabasin	Dextral oblique. Up to the east	Qipc
K	Approximately located, concealed, and queried	3.4 – 5.1	N15°W – N5°E	Mountain front to proximal	Sinistral oblique?	QToa
L	Queried	3.2	N45°E	Mid fan	Normal?	Qoa?
M	Certain and concealed	1.4	N75°E	Distal fan to valley axis	Normal, down to the north. Aligned with bedrock shear zone	Qoa
N	Approximately located	1.5	N55°E	Mountain front	Normal, down to the	Qoa

O	Queried	0.6	N45°W	Mountain front	south? ?	Qia
P	Approximately located, concealed, and queried	0.3 – 6.4	~N10°W	Mountain front to proximal fan	Normal	Qoag
Q	Certain, approximately located, concealed, and queried	2.5	~N20°W	Mountain front to proximal fan	Normal	Qoa
Fold ID	Reliability of location	Length (km)	Average strike	Geomorphic expression	Sense of movement	Age of youngest faulted deposit
A	Approximately located	7	~N45W	Low amplitude folding of late Pleistocene deposits.	Assymmetric anticlinal, plunging south 5 degrees	Qig
Q	Inferred	5.1	N 85° E	Mountain front to distal fan	Anticlinal	Qoa?